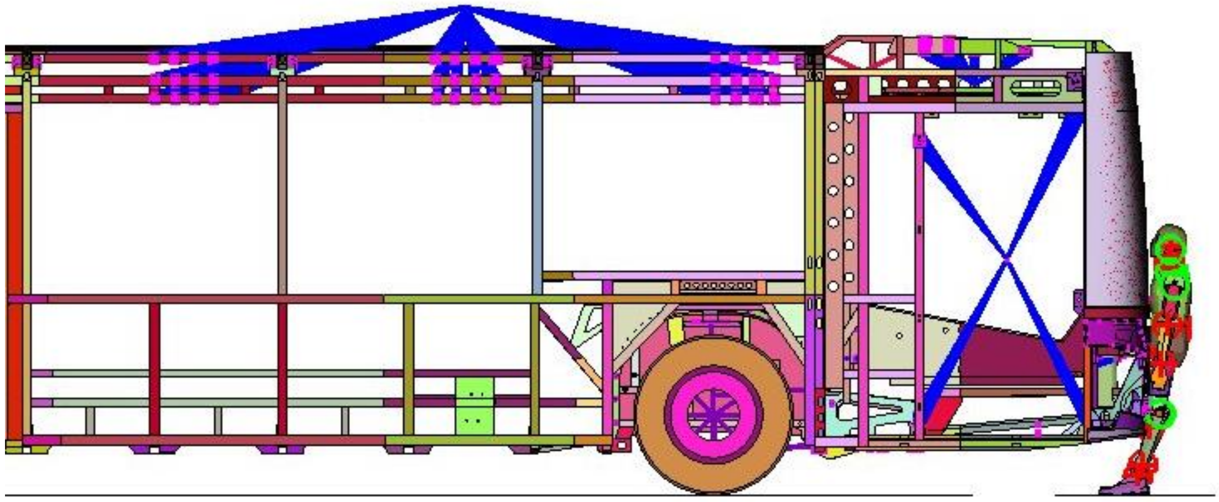

Vulnerable Road User head impact evaluation for bus front ends using Finite element model

Master's thesis in Automotive Engineering

ADITYA SHASHIKANT PUJARI

DEPARTMENT OF MECHANICS AND MARITME SCIENCES
CHALMERS UNIVERSITY OF TECHNOLOGY

Gothenburg, Sweden 2022
www.chalmers.se

MASTER'S THESIS AUTOMOTIVE ENGINEERING

VRU Head impact evaluation for bus front ends using Finite element model

ADITYA SHASHIKANT PUJARI

Department of Mechanics and Maritime Sciences
Division of Vehicle safety
CHALMERS UNIVERSITY OF TECHNOLOGY
Göteborg, Sweden 2022

VRU Head impact evaluation for bus front ends using Finite element model
ADITYA SHASHIKANT PUJARI

Master's Thesis 2022:66
Department of Mechanics and Maritime Sciences
Division of Vehicle safety
Chalmers University of Technology
SE-412 96 Göteborg
Sweden
Telephone: + 46 (0)31-772 1000

Cover:
Simulation of the bus model colliding with the dummy human model

Department of Mechanics and Maritime Sciences
Göteborg, Sweden 2022-10-15

VRU Head impact evaluation for bus front ends using Finite element model

Master's thesis in master's Automotive Engineering
ADITYA SHASHIKANT PUJARI
Department of Mechanics and Maritime Sciences
Division of Vehicle safety
[Company Address]
Chalmers University of Technology

Abstract

Numerical studies in crashworthiness have played an important role in optimizing vehicle design and making them pedestrian friendly. The developments seen in passenger vehicle exceeds the developments in bus when concerning pedestrian safety. Head injury is one of the most frequently sustained injuries during an impact between a bus and a pedestrian and these typically result in a 20% fatality rate. The impact may produce pure linear acceleration of the head but typically also produce rotation acceleration of the head. The head kinematics are known to highly influence the type of resulting head injuries. In this master's thesis, head to bus front impacts were simulated and the responses were evaluated to study the effect of head impact location, orientation, and velocity on head kinematics and injury risks. Finite Element (FE) models of a free-motion head form and a Hybrid III 50th percentile male crash test dummy and a of a naked frame of Scania low-entry comfort bus with attached front windscreen and plastic panel were used in this study. The Head Injury Criteria, Rotational Injury Criteria, and the Power Rotational Head Injury Criteria were used to estimate the injury risks. The resulting injury risks based on linear accelerations were similar for the simulated impacts when the human head was represented by the free-motion headform and the human was represented by the Hybrid III model. Since the estimated head injury based on rotational accelerations were rather high the Hybrid III is the recommended tool for bus front head injury risk estimations.

Key words:

Head impact, Injury criteria, Free motion headform, Hybrid III dummy, Crash test, Skull fracture, Traumatic brain injury, Bus

Contents

Preface

The work presented in this master thesis was conducted at Scania technical centre, Södertalje between January 2022 and August 2022. This work was a collaboration between Chalmers technical university and Scania bus development.
First, I would like to thank my supervisor Professor Johan Davidson from Chalmers University for his support and encouragement. I also would like to thank my industrial supervisors Dr. Mohammad Shirzadegan and senior engineer Nilesh Dharwadkar for their valuable inputs and support.
At the end I would like to express my appreciation to my lovely family for their all-time support.

Göteborg March 2022-10-15

ADITYA SHASHIKANT PUJARI

Notations

α_t	resultant angular acceleration
α_i	angular acceleration in ‘i' direction (i=x,y,z)
α_{cr}	critical angular acceleration
ω_{cr}	critical angular velocity
ω_{max}	maximum angular velocity
ω_x	maximum angular velocity in the x direction
ω_y	maximum angular velocity in the y direction
ω_z	maximum angular velocity in the z direction
ω_{xcr}	critical angular acceleration in the x direction
ω_{ycr}	critical angular acceleration in the y direction
ω_{zcr}	critical angular acceleration in the z direction
ω_r	maximum angular resultant velocity
θ_{brain}	peak relative brain angle
$a(t)$	resultant linear acceleration
a_i	linear acceleration
c	damping coefficient
k	stiffness coefficient
I_{ii}	moment of inertia in ‘i' direction
m	mass of the head
t_1	the initial integral time over which injury criteria is calculated
t_2	final integral time over which injury criteria is calculated

Abbreviations

VRU	Vulnerable road user
CV	Commercial Vehicle
CoG	Centre of Gravity
HIC	Head injury criteria
U S	United states
mTBI	Mild Traumatic brain injury
sTBI	Severe Traumatic brain injury
RIC	Rotational injury criteria
PRHIC	Power rotational head injury criteria
HIP	Head impact power
BRIC	Kinematic rotational brain injury criterion
BrIC	Brain Rotational injury criterion
KLC	Kleivin's linear combination
BAM	Brain angle metric
LE	Low entry
LF	Low floor
LSTC	Livermore software technology corporation
NHTSA	National highway traffic safety administration
FMVSS	Federal motor vehicle safety standard
FMH	Free motion headform
BITS	Bus impact test score

1 Introduction

This master's thesis involves evaluation of vulnerable road user's head impact with respect to the bus front end. The study involves simulation of collision of the finite element model of the city bus with the finite element model of free motion head form and the finite element model of the city bus with finite element model of the hybrid III 50^{th} percentile male dummy. The model used in this study is of a comfort bus with a low entry developed by Scania CV AB, hereafter referred to as the Low entry comfort bus.

The boundary conditions such as contact friction and impact velocity chosen are based on previously conducted experiments /simulations. Critical impact locations on the bus front structure are located for the heights other than the height of the hybrid III 50^{th} percentile male model. The orientation of the hybrid III 50^{th} percentile male model with respect to the bus front is also taken into consideration. The kinematics at the head CoG such as maximum linear acceleration and velocity (from both free motion head form and Hybrid III dummy) in all the three directions and maximum angular acceleration and velocity (from only Hybrid III dummy) in all the three directions are gathered and different head injury criteria is calculated.

The evaluation of head impact is very important as there is not only the possibility of visible injury like skull fracture but also other brain injuries that is not visible such as, traumatic brain injuries. There have been many efforts taken in the department of active safety to ensure vulnerable road user's protection. But There is no such regulation, that ensures the safety of the pedestrians during the bus impact. However, Transport for London buses has suggested Free motion head impact test on the windscreen. The test involves impact on the windscreen at specified locations on the windscreen and calculate of the head injury criteria (HIC_{15}) using the linear acceleration values obtained from the accelerometer installed at the centre of gravity of the free motion head form. Based on the HIC_{15} values obtained, points are provided, and the safety rating is given to the bus [23]. Scania would like to understand the implications of the test in case the regulations are mandated globally. Hence, this thesis will provide a good starting point to set-up a test method and calculation of injury criteria. The point to be noted was that crash data of pedestrian with the bus is not available publicly and validation of the simulation results were found to be challenging. The statistics presented in the upcoming sections does not give a complete picture of the crash. In some of the data found the fatality rate is mentioned but it is not clear if the fatality is concerning pedestrian or the occupants of the bus.

The free motion headform used in this study are equivalent to the head of 50^{th} percentile male model. The hybrid III 50^{th} percentile male dummy model used are sometimes mentioned as just hybrid III dummy in the report. This study will aim to understand the injury associated with collision of Low entry comfort buses and measure required injury criteria.

2 Background

2.1 Crash Statistics

According to European road safety observatory, of bus crashes in 2019, the fatality of the pedestrian accounted for 29% of the 521 fatalities reported. Hence, about 150 people were pedestrians impacted by a bus [27]. In India 2020, fatalities involving pedestrians increased by 16% from previous year, but the proportion of fatalities involving a crash with a bus was unclear [28].

According to WHO global status report in 2018 on road safety, 1.35 million fatalities per annum are due to road traffic accidents which accounts to 2.5% of the total fatalities and about 20-50 million serious injuries are sustained in crashes globally [15]. Figure 1 shows the comparison of fatalities in 2010 and 2019 in the USA, where there has been an increase in share of fatalities involving pedestrians from 15% to 20%. Looking at the injuries sustained by pedestrians, there was an increase of 1.3% in the number of pedestrians injured in 2018 from 75,000 to 76,000 in 2019 in the USA.

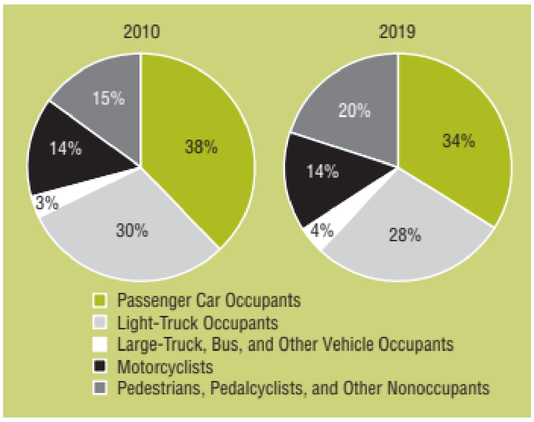

Figure 1: Fatality composition (by Road user category) for 2010 and 2019 [16]

Unprotected road users (URU) fatalities have increased from 20% in 1996 to 34% in 2019 in the USA [16]. With the upcoming sensor technology improving, road traffic accidents are expected to reduce. Table 1 shows some statistical data that compares fatal bus crash scenarios with different types of vehicles.

As shown in Table 1, of all the bus accidents, impacts with pedestrians accounted for about 3.7%. Fatalities of pedestrians during bus crashes accounted for 22.5% in the USA [17]. Looking at the data post 2020 would not give us relevant statistics due to decrease in activities because of COVID-19.

According to road accidents in India 2020, 57,763 pedestrians were involved in road accidents, comprising 15.8% of the total share of accidents. There were 23,477 fatalities among pedestrians accounting for 17.8% of the total fatalities [28]. Table 2 shows the distribution of pedestrian fatalities with different types of vehicles. Of the 23,477 fatalities 1,161 cases were caused by impact with the buses [28].

Table 1: Vehicles involved, persons involved, and persons killed in fatal bus crashes in US, 2019 [17]

Vehicle/Person Type	**Vehicles Involved**		**Persons Involved**		**Persons Killed**	
	Number	**Percent**	**Number**	**Percent**	**Number**	**Percent**
Vehicle/Vehicle Occupants						
Passenger Car	91	19.9%	136	8.1%	69	26.7%
Light truck	91	19.9%	133	7.9%	51	19.8%
Large truck	17	3.7%	25	1.5%	5	1.9%
Bus (Single vehicle crash)	78	17.0%	373	22.1%	17	6.6%
Bus (Multiple vehicle crash)	154	33.6%	908	53.9%	18	7.0%
Motorcycle	23	5.0%	24	1.4%	24	9.3%
Other vehicle type	4	0.9%	2	0.1%	1	0.4%
Total Vehicles/Vehicle Occupants	**458**	**100.0%**	**1601**	**95.0%**	**185**	**71.7%**
Non-motorists						
Occupant of a motor vehicle not in transport	-	-	6	0.4%	0	0.0%
Occupant of a Non-motor vehicle transport device	-	-	0	0.0%	0	0.0%
Pedestrian	-	-	63	3.7%	58	22.5%
Bicyclist	-	-	12	0.7%	12	4.7%
Person on a personal conveyance	-	-	3	0.2%	3	1.2%
Person in or on a building	-	-	0	0.0%	0	0.0%
Total Non-Motorists	**-**	**-**	**84**	**5.0%**	**73**	**28.3%**
Total	**458**	**100.0%**	**1685**	**100.0%**	**258**	**100.0%**

According to European road safety observatory, majority of the road fatalities occur on road stretches. The case of fatalities in bus crash, about 72% of all fatalities occurred on a road stretch [27]. The common position of pedestrian would be facing perpendicular to the bus and sometimes react in shock and face the bus [32]. The impact location can be anywhere on the bus front end and hence, performing simulation at the weakest impact location was a good place to start.

Table 2: Distribution of fatalities of pedestrians involving different types of vehicles

Vehicle type	**Pedestrian Fatality (2020)**	
	Number of deaths	**Share in total**
Bicycles	107	0.45
Two wheelers	6,489	27.63
Auto Rickshaws	954	4.06
Cars, Taxi, Vans & LMV	5,511	23.47
Trucks/ Lorries	4,142	17.64
Buses	1,161	4.94
Other Non/motorized vehicle (E-rickshaw etc.)	305	1.29
Others	4808	20.48
Total	**23477**	**100**

2.2 Traumatic Brain Injuries

The injury sustained by a pedestrian will be dependent on the position of the pedestrian with respect to the bus [32]. Injuries can range from broken bones in the extremities, neck injuries, thorax injuries, pelvis injuries, and traumatic brain injuries. Traumatic brain injuries are very common when it comes to pedestrian-vehicle crashes [18]. The impact caused when the pedestrian collides with a passenger vehicle is relatively different from an impact with flat front vehicles. The main difference being the time taken for the head impact relative to the first point of contact.

Traumatic brain injuries are considered to be an “invisible epidemic” as most of the time it is not readily apparent to others. A Broader concept discussed is Head injury. The main difference between Head injury and Brain injury is that no brain tissue is damaged in a head injury. Brain injuries can have adverse effects. It is very important to predict head injuries, as the brain cannot be deformed without causing injury and a possibility of permanent damage.

2.2.1 Symptoms

The short-term symptoms, in case of mild brain injury, one might experience Headache, confusion, dizziness, sensory problems, mood changes, concentration problems, and unconsciousness. In case of severe brain injury, one might experience constant headache, Nausea, dilated pupils, loss of coordination, Increased confusion, and numbness. The long-term symptoms include memory loss, lack of concentration, sensory impairments, motor impairments etc.

The above-mentioned reasons apart from imminent death are the reasons why it is important to predict brain injury.

2.2.2 Injury Mechanism

During the head impact, the direction of loading determines the injury mechanism as mentioned below.

- **Direct loading**
    - Linear Acceleration
        1. Deformation and fracture
        2. Stress waves
        3. Pressure gradients
        4. Indirect fracture
    - Rotational Acceleration
        1. Relative motion between skull and brain
        2. Shear in brain tissue
- **Indirect loading**
    - Rotational acceleration due to inertia
        1. Relative motion between skull and brain

An observation was made where most of the TBI’s could be explained using rotation between skull and brain. It was noted that translations were not as harmful as rotations [20].

2.2.3 Types of TBI’s

An article by MEA Forensic Engineers and Scientists, INC. suggests that the most common type of head injuries sustained during a crash include skull fracture, contusion, concussion, diffuse axonal injury, subdural hematoma, and subarachnoid hematoma [19].

Table 3: Classification of Traumatic Brain Injury

Traumatic Brain Injury				
Focal Brain Injury			**Diffuse Brain Injury**	
Contusion	**Hematoma**	**Laceration**	**Axonal**	**Concussion**
	Epidural		Mild	Mild
	Subdural		Moderate	Classic
	Subarachnoid		Sever	
	Intracerebral			

2.3 Injury Risk Prediction

This chapter illustrates equations, variables, and parameters, that are used in the injury prediction criteria. These equations are associated with linear and rotational accelerations.

2.3.1 Associated with linear acceleration

2.3.1.1 Head injury criteria (HIC)

The Head injury criteria is a measure of the probability of skull fracture during the crash scenario. It is developed initially by Gurdjian et al. and has been evolving since [31], It is calculated using Equation 1, which is a function of resultant linear acceleration for specific duration.

$$HIC = \left[(t_2 - t_1)\{\frac{1}{t_2 - t_1}) \int_{t_1}^{t_2} a(t)dt\}^{2.5}\right]_{\max} \quad \text{Equation 1}$$

Where *a(t)* is the resultant linear acceleration and t_1 and t_2 are the initial and final integral time over which HIC is calculated. According to the current automotive standard, t_2-$t_1 \leq 15$ milliseconds [10]. A head injury risk curve was developed by Prasad et al. using cadaver impact test to determine the severity of the impact. The severity is measured on abbreviated injury scale (AIS) ranging from 0 to 6. Where 0 denotes no injury and 6 denotes unsurvivable injury [9]. This helps in estimation of risk of a specific injury. A HIC_{15} of 700 was estimated as a 5% risk of Abbreviated Injury Scale (AIS) 4+ head injury (skull fracture) [11].

2.3.2 Associated with rotational acceleration

The below mentioned injury criteria's will be used for the study as their corresponding threshold value is available

2.3.2.1 Rotational injury criteria (RIC)

The Rotational injury criteria is a measure of the probability of TBI during the crash scenario and it was presented by Ommaya et al (1967) [30]. It is calculated using Equation 2, which is a function of resultant rotational acceleration for specific duration.

$$RIC = \left[(t_2 - t_1)\{\frac{1}{t_2 - t_1}) \int_{t_1}^{t_2} \alpha(t)dt\}^{2.5}\right]_{\max} \quad \text{Equation 2}$$

Where α_t is the resultant angular acceleration.

2.3.2.2 Power rotational head injury criteria (PRHIC)

The Power rotational head injury criteria are also a measure of the probability of TBI during the crash scenario and it was presented by Newman in 2000 [29]. It is calculated using Equation 3, which is a function of rotational part of HIP provided in Equation 4.

$$PRHIC = \left[(t_2 - t_1)\{\frac{1}{t_2 - t_1}) \int_{t_1}^{t_2} HIP_{rot}\ dt\}^{2.5}\right]_{\max} \quad \text{Equation 3}$$

$$HIP = \sum m.a_i\ .\int a_i\ dt + \sum I_{ii}.\alpha_i\ .\int \alpha_i\ dt \quad \text{Equation 4}$$

Where HIP_{rot} is the rotational part of the total HIP, m is he mass of the head, a_i is the linear acceleration, I_{ii} is moment of inertia and α_i angular acceleration.

2.3.2.3 Other notable injury criteria

These are some noteworthy injury criteria's. These will not be used in the study due to lack of threshold values.

2.3.2.3.1 Kinematic rotational brain injury criterion (BRIC)

Kinematic rotational brain injury criterion was proposed in 1940's to predict brain injury [12]. It was calculated using Equation 5.

$$BRIC = \frac{\omega_{max}}{\omega_{cr}} + \frac{\alpha_{max}}{\alpha_{cr}} \quad \text{Equation 5}$$

Where ω_{cr} is the critical angular velocity, α_{cr} is the critical angular acceleration, ω_{max} is maximum angular velocity and α_{cr} is maximum angular acceleration. The critical values are different for different ATD's [12].

2.3.2.3.2 Brain rotational injury criterion (BrIC)

Brain rotational injury criterion is developed to account for diffuse axonal injury [13]. It is calculated using Equation 6.

$$BrIC = \sqrt{(\frac{\omega_x}{\omega_{xcr}})^2 + (\frac{\omega_y}{\omega_{ycr}})^2 + (\frac{\omega_z}{\omega_{zcr}})^2} \quad \text{Equation 6}$$

Where [ω_x ω_y ω_z] are the maximum angular velocities in the three spatial direction and [ω_{xcr} ω_{ycr} ω_{zcr}] are the critical angular acceleration for the same [13].

2.3.3 Associated with both linear and rotational acceleration

2.3.3.1 Kleivin's linear combination (KLC)

Kleivin's linear combination developed by Kleivin, predicts brain injury using a linear combination of HIC_{36} and maximum angular velocity as shown in Equation 7 [6].

$$KLC = 0.004718.\omega_r + 0.000224\,.HIC_{36} \quad \text{Equation 7}$$

Where ω_r is the maximum angular resultant velocity.

2.3.4 Associated with brain tissue deformation

2.3.4.1 Brain angle metric (BAM)

Brain angle metric is a metric used to classify between injurious and non-injurious impacts. It was suggested by Laksari et al (2019) [14]. It is calculated using Equation 8.

$$I.\left(\ddot{\theta}_{brain} + \ddot{\theta}_{skull}\right) = -k.\theta_{brain} - c.\dot{\theta}_{brain} \quad \text{Equation 8}$$

Where θ_{brain} is peak relative brain angle, k is the stiffness coefficient and c is the damping coefficient [14].

The injury criteria's that will be used in the study are Head injury criteria, Rotational injury criteria and Power rotational head injury criteria. The reason for selecting these injury criteria's is because of the relevant threshold values available to understand the severity of the injury.

2.4 Threshold

According to Kaveh Laksari et al. the HIC is a good predictor of skull fracture [14]. Based on Dokko et al. [8], threshold values of the injury criteria's RIC and PRHIC are considered. Following some more literature, according to Kimpara et al. RIC is a good predictor of mild traumatic brain injury (mTBI) whereas PRHIC is a good predictor of severe traumatic brain injury (sTBI) [6]. The threshold values mentioned in Table 4, predicts a 50% probability of mTBI and not sTBI [6]. These threshold values are derived from both concussive and non-concussive data obtained from the National football league (NFL). The head impact occurring during NFL is not as severe as pedestrian crash and hence there is no threshold value for injury criteria associated with sTBI.

The threshold value used in this study for HIC is that typically used in automotive standards [11]. The values are presented in Table 4.

Table 4: Threshold values of certain injury criteria's

Injury criteria	Threshold value	Outcome
HIC	1000	Skull fracture
RIC	1.03×10^7	50% probability of mTBI
PRHIC	8.70×10^5	50% probability of mTBI

2.5 Transport for London bus

There is no regulation regarding the front stiffness of the bus when it comes to pedestrian impact. However, a reference can be found on transport for London buses. The specifications are laid for all the new London buses. The documents suggest the front structure of the buses to have arrangements to absorb the energy during an impact, to improve the protection of the VRUs.

The documents suggest a test method to provide scores to the bus and provide the safety rating. The test involves a FMH being projected on the windscreen of the bus at different locations. The acceleration values are recorded and the HIC_{15} is calculated. The impact location is divided along with the windshield as shown in Figure 2. The requirement for the bus fleets rolled out from 2024 is that the head form impact test performed should not exceed HIC_{15} above 1350. Test is conducted at 40 kmph. The scoring criteria are called Bus VRU impact test performance scores (BITS),

1) HIC<700 = 2 points

2) 700 ≤ HIC ≤1000 = 1 points

3) HIC > 1000 = 0 points

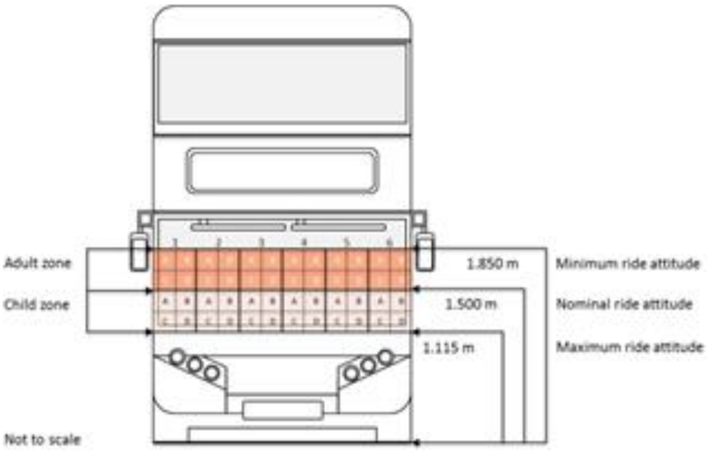

Figure 2: Impact location on the bus front structure [24]

Of the 24 impact areas that are tested with at least 25% of areas need to be safe for the bus to pass the test [23].
This document gives a good understanding of the test that is performed. The impact velocity of 40 km/h is high and lies at the tail end of the spectrum. The thesis work has just used this document as a reference and will not adhere completely to this document. The impact area can be broadened to cover regions other than the windscreen.

2.6 Scania

Scania is a provider of transport solutions, including trucks and buses for heavy transport applications offering [22]. The buses provided by the company are-

- Scania citywide LF (low floor)
- Scania citywide LE (low entry)
- Scania interlink
- Scania Touring HD
- Scania Irizar- i6, i6s & i8

Scania citywide LE (low entry) chosen for the study, is shown in Figure 3. As mentioned in the previous chapter, most of the pedestrian crashes are expected to occur within the city limits and this city bus is ideal to understand the implications of a pedestrian crash. Thus, Scania would like to understand the head injury occurring during a pedestrian impact with the bus front end.

Transport for London buses has suggested passing criteria for the bus, where a free motion headform impact test on the windscreen should result in Head injury criteria not greater than 1350 [23]. By means of free motion head form, the required impact test can be performed, then with the help of linear acceleration, the HIC_{15} is calculated. Moreover, the Hybrid III 50th percentile male dummy model is used to further perform crash tests and calculate injury criteria associated with rotational acceleration. The model is also used to study the relative positioning of the dummy with the bus.

Figure 3: Scania Citywide Low entry comfort bus [22]

3 Method

This section will describe the different FE model and the boundary conditions used for FE representation of the head impact and to perform simulations in LS-Dyna.

3.1 Finite element model

This chapter explains a summary of the finite element models that have been used in this study. Note that, the mathematical explanation behind the FEM is beyond the scope of this work. Thus, they are not presented here.

3.1.1 Model of the free motion headform

The Free motion head form (FMH) is a hybrid III 50th percentile dummy type head model. This was used to determine the risk of head injury when the head contacts a structure in a collision. When it was used, it was projected on a defined section of a vehicle structure and the head centre of gravity acceleration are recorded by the use of accelerometers in the headform. The acceleration signals can be used to calculate the HIC but not any rotational injury criteria. The FE model of the FMH used for the study is developed by Livermore Software Technology Corporation (FMH.091201_V2.0, LSTC). Figure 4 shows a schematic view of the FMH.

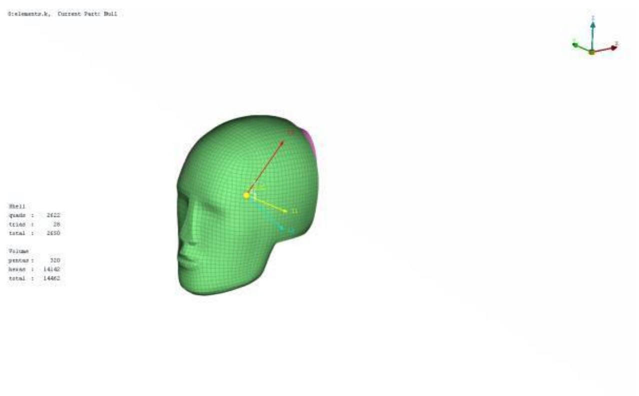

Figure 4: Free motion head form model from LSTC.

3.1.2 Model of the Hybrid III 50 Percentile Male ATD

The Hybrid III 50th percentile male anthropometric test dummy (ATD), hereafter referred to as Hybrid III, was developed for use in vehicle frontal crash testing and instrumented in such a way as to provide HIC values in crash tests [3].

The Hybrid III 50th percentile male FE model is also developed by Livermore Software Technology Corporation (H3_50TH_STANDING.100630_BETA, LSTC). It is based on the respective Hybrid III anthropomorphic test dummy. Figure 5 shows a schematic view of the Hybrid III dummy used.

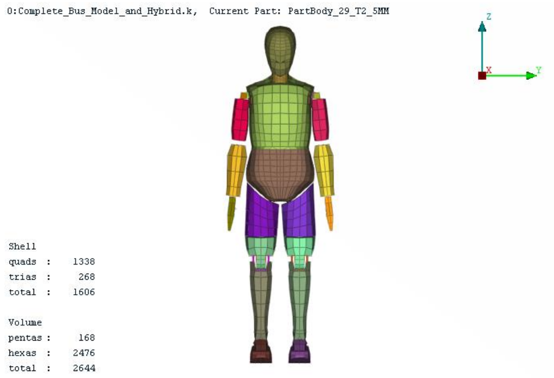

Figure 5: Hybrid III 50th percentile male dummy model from LSTC.

The specification of the head of a Hybrid III 50th percentile male dummy is as follows, these values are needed to calculate injury predictors.

i. Mass- 4.728 kg
ii. Principal moments of head inertia in x direction (kg.m^2) I_{xx}=24526.1 × 10^{-6}
iii. Principal moments of head inertia in y direction (kg.m^2) I_{yy}=22107.2 × 10^{-6}
iv. Principal moments of head inertia in z direction (kg.m^2) I_{zz}=16355.2 × 10^{-6}

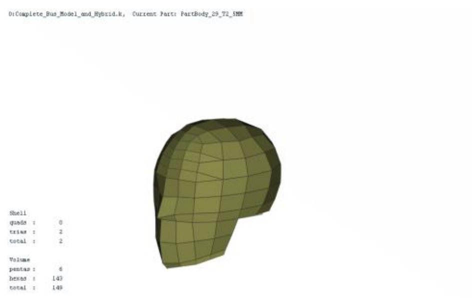

Figure 6: Head of Hybrid III 50th percentile male dummy model

3.1.3 Model of the Citywide Low Entry Comfort Bus

The FE model of the LE comfort bus developed at Scania is shown in Figure 7. The overall length was 14.5m. The superstructure of the body was mounted on a ladder frame chassis. The geometry was modelled in ANSA. The calculations are made in LS-DYNA software. The geometry was modelled with a mix of solid elements, shell elements and beam elements. The bus body superstructure, chassis modules, suspension and powertrain masses are included in the FEA model as per Scania methodology.

The seat and the passenger weight were modelled as a point mass at the H point of the seat or at the CoG position of a two-seater bench seat. The point mass was then connected to the seat attachment points on the floor. The front windscreen and plastic panel are further attached. Figure 7 shows the side view of the superstructure where the weight of the roof and door are replaced by a point mass.

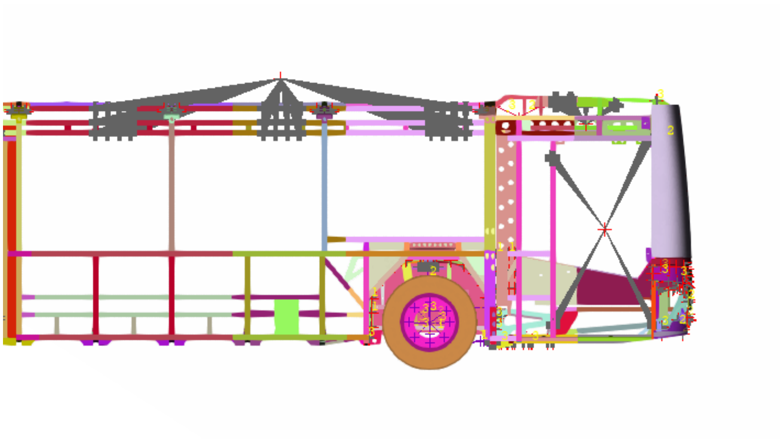

Figure 7: Side view of Superstructure of Scania LE comfort bus

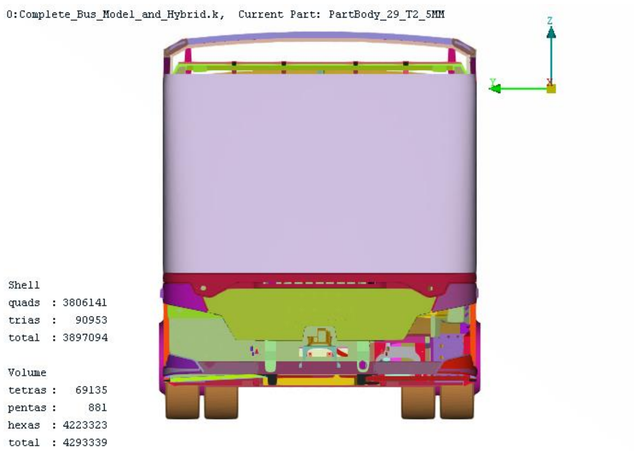

Figure 8: Front view of Superstructure of Scania LE comfort bus

In this work, to reduce the computations time, the rear end of the bus was removed, and an equivalent point mass was placed at the centre of gravity of the removed section. This point mass was connected to the rest of the bus. The point mass was constrained in y and z direction transitionally. This arrangement does not have any impact on the kinematics of the crash. The computational time was reduced by approximately one hour. Figure 9 shows the FE model that was used in this study.

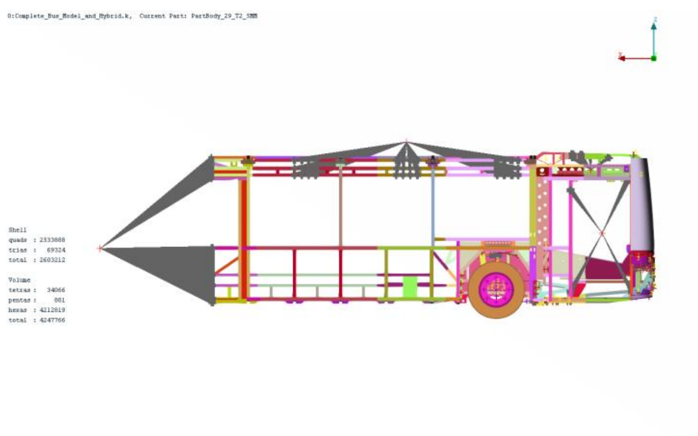

Figure 9: Side view of reduced model of Scania LE comfort bus

3.1.3.1 Front part

Usually, the front model of the bus consists of several parts. Here, a summary of the windscreen and plastic panel are addressed.

3.1.3.1.1 Windscreen

The windscreen was modelled as shown in Figure 10. The different layers of the windscreen are

1. Windscreen support -
   Material card- MAT1
2. Windscreen lamination
   Material card- MAT123
   MAT_MODIFIED_PIECEWISE_LINEAR_PLASTICITY
3. Windscreen glass
   Material card- MAT1
4. Windscreen lamination
   Material card- MAT123
   MAT_MODIFIED_PIECEWISE_LINEAR_PLASTICITY

A tie contact between each layer of the windscreen was defined. Static coefficient of friction was set to be 0.15 and dynamic coefficient of friction was set to be 0.08. Figure 10 shows the exploded view of the windscreen.

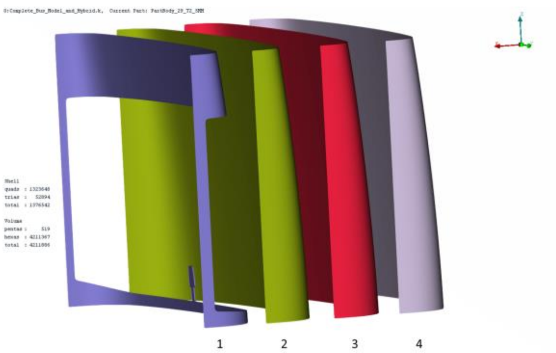

Figure 10: Windscreen exploded layers view

3.1.3.2 Plastic panel

The plastic panels shown in Figure 10. Are the ones considered for the study. These are the panels that have the potential area of impact in some of the crash scenarios. The material used was MAT24 with density of 9.05×10^{-7} kg/mm^3.

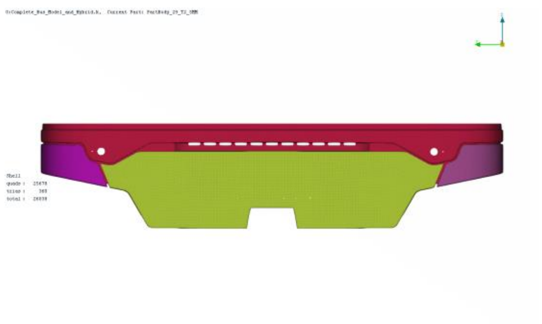

Figure 11: Front plastic panel under consideration

The plastic panel was glued to its front supporting structure by providing an adhesive type of connection. The front supporting structure is made of Steel and its properties are mentioned in Table 5. The glue line is highlighted in Figure 12.

Figure 12: Adhesive contact between the plastic panel and front supporting structure

Linear-plastic material model was used to show the material behavior of the windscreen, front plastic panel and bumper. The failure mode from the windscreen model was disabled, as there was no physical test data available to verify the failure model of the material for the impact test. This was done by assigning the value of plane strain at failure to be 0 in the material card. The properties are mentioned Table 5.

Table 5: Material properties of the bus front structure.

	Mass density (kg/mm^3)	Young's modulus (Gpa)	Poisson's ratio
Windscreen glass	2.70×10^{-6}	90	0.23
Windscreen lamination	1.21×10^{-6}	2	0.31
Front plastic panel	9.05×10^{-7}	1.3523	0.40
Front supporting structure	7.85×10^{-6}	210	0.30

3.1.4 Finite element model set up

The model of the bus was placed on a rigid ground surface. The contacts were provided between the tires and the ground as shown in Figure 13. The friction between ground and tire was set to be 0.6 [25].

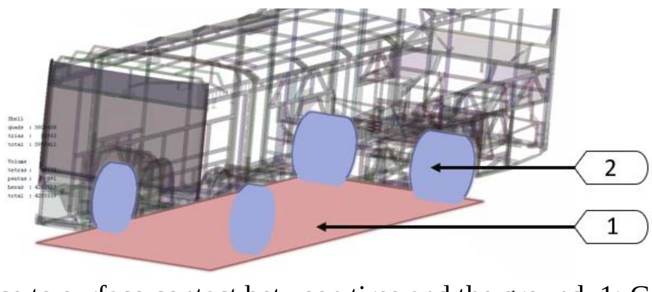

Figure 13: Surface to surface contact between tires and the ground, 1: Ground-Master, 2: Tires-Slave

The highlighted part in Figure 14 shows parts to which global contacts are provided to avoid self-penetration. The friction values were set to be 0.15.

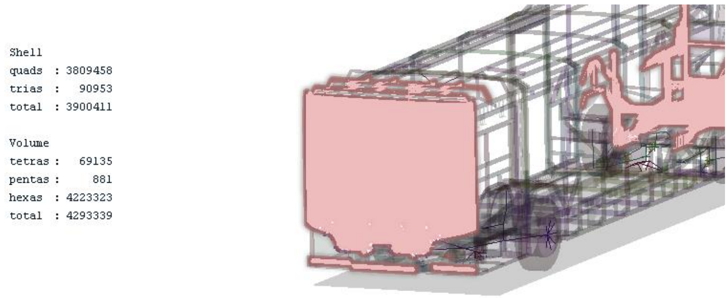

Figure 14: Global contacts of the model of the bus members

3.1.4.1 Free motion headform and the model of the bus

The impact test performed between the free motion head form and the model of the bus is slightly different from the testing conditions in real life. In the simulation model, the FMH is given constant velocity in the x- direction. The acceleration is recorded at the CoG of the head to understand the behavior during the impact. The impact test setup is shown in Figure 15.

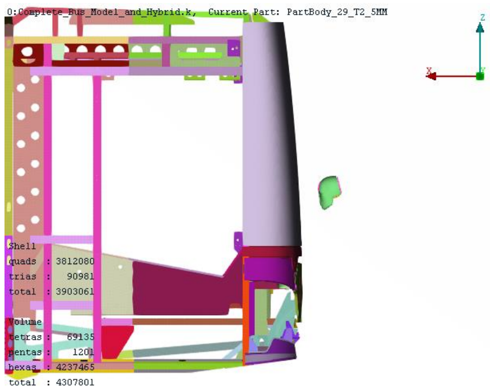

Figure 15: FMH and the bus model impact setup

The contact was provided between the outermost layer of the FMH and the frontal area of the model of the bus as shown in Figure 16. The automatic surface to surface type contact was provided between the two with coefficient of friction to be 0.3 [25]. The direction of the velocity was provided to all the nodes of the FMH model as shown in Figure 17.

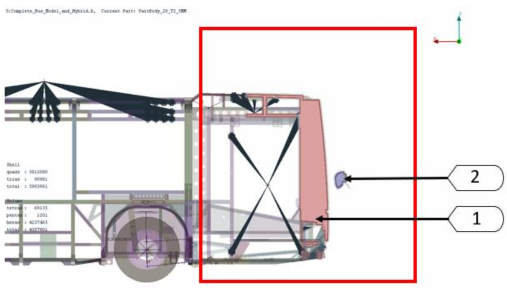

Figure 16: Contact between the FMH and the bus model, 1: The frontal area of the model of the bus- Master, 2: FMH- Slave

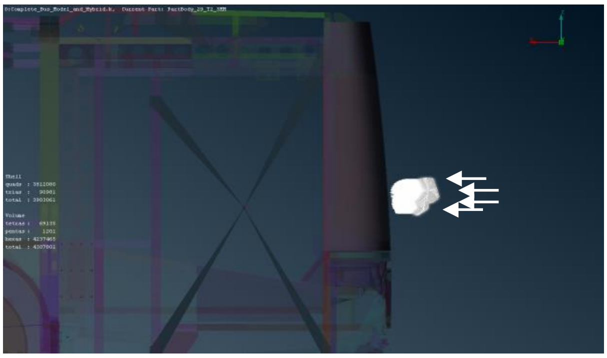

Figure 17: Direction of the velocity provided to the FMH

3.1.4.2 Hybrid III 50th percentile male dummy and the model of the bus

The Hybrid III dummy was also placed on the ground. An automatic surface to surface contact was provided between the foot of the Hybrid III dummy and the ground with the coefficient of friction of 0.6 as shown in Figure 18 [25].

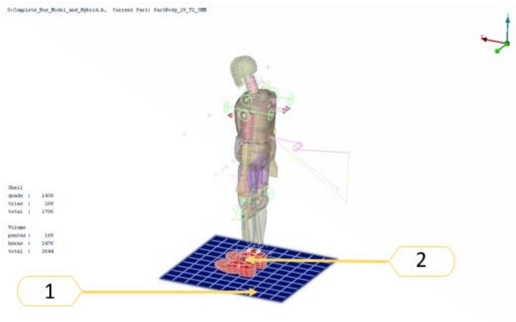

Figure 18: Contact between Hybrid III dummy and ground, 1: Ground-Slave, 2: Hybrid III dummy foot- Master

The setup of the impact test between the Hybrid III dummy and the model of the bus is shown in Figure 19. An automatic surface to surface contact is provided between outer layers of Hybrid III dummy and the front section of the model of the bus with a coefficient of friction of 0.3 as shown in Figure 20 [16]. The neck was excluded from the outermost section of the Hybrid III dummy because the model does not have failure mode and there won't be any penetration.

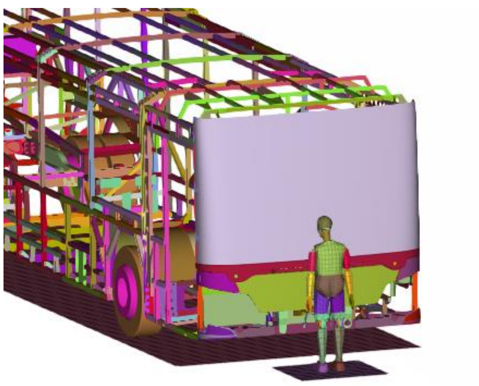

Figure 19: Hybrid III dummy and the bus impact setup

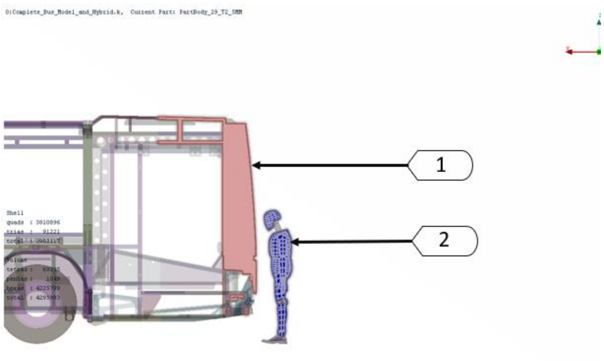

Figure 20: Contact between the Hybrid III dummy model and the bus model, 1: The frontal area of the model of the bus- Master, 2: Hybrid III dummy model- Slave

Unlike the impact test performed using the FMH and the model of the bus where the velocity was provided to each node of the FMH, during the impact test between the Hybrid III dummy, the direction of the velocity was provided to all the nodes of the bus model as shown in Figure 21. This resembled the actual impact scenario.

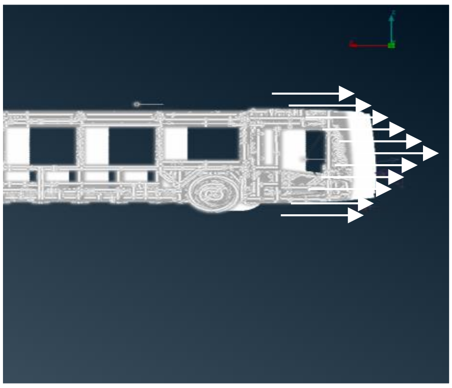

Figure 21: Direction of the velocity provided to the bus model

3.2 Software used

The software used during this master's thesis include the pre-processor ANSA and Ls-dyna deck and the post-processor META developed by BETA CAE systems. The post-processing in META provides the calculation of the Head injury criteria. Obtaining just HIC_{15} may not be sufficient for the study as it depicts only the possibility of the skull fracture, hence, we also need to measure injury criteria that predict traumatic brain injuries.
MATLAB code is written to calculate different injury criteria values based on the values obtained from the post processing of the simulation.

3.3 Boundary Conditions for the simulation set up

For the simulation test involving impact between the FMH and the bus,

- The FMH is impacted on the bus front structure at the velocity of 18 km/h, 26 km/h and 40 km/h.
- The height of the CoG of the FMH from the ground is set to be 0.976 m, 1.096 m and 1.576 m.

For the simulation test involving impact between the Hybrid III dummy and the bus,

- The bus is impacted with the dummy at the velocity of 18 km/h, 26 km/h (Not at 40 km/h because of the results obtained from FMH test).
- The height of the CoG of the head of the Hybrid III dummy from the ground is set to be 0.976 m, 1.096 m, and 1.576 m.
- The Hybrid III dummy with respect to the bus is positioned at 0° and 90°.

The orientation of the Hybrid III dummy is finalized by performing a rigid wall crash test with the Hybrid III dummy. The orientation of the wall with respect to the hybrid III dummy was set to 0°, 30°, 45°, 60°, 90° and 180°. The impact velocity is set to 18 km/h and the friction contact is like the values used in defining the contact between the bus and the hybrid III dummy. The result is discussed in Appendix I.

For the above tests conducted, the failure mode is disabled in the material model used for the windscreen. A comparison is done between the FMH impact test and Hybrid III dummy impact test, where the height of the head CoG from the ground is 1.576m and the impact velocity is 26 km/h. This test has failure mode enabled in the material card of the windscreen. The results are shown in Appendix III.

To understand the significance of the supporting structure behind the front panel, the stiffness of the sheet metal structure is reduced by reducing its thickness and the simulation performed. The part whose thickness is reduced is shown in Figure 22. The test involves the hybrid III dummy impact at the velocity of 26 km/h. The height of the head CoG from the ground is 0.976 m.

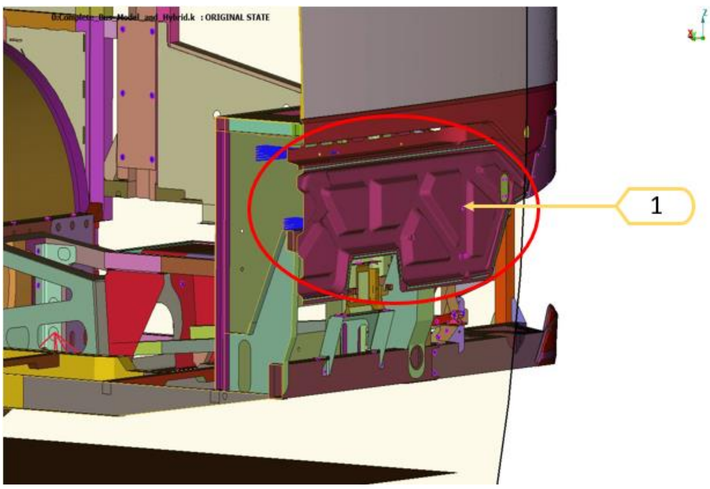

Figure 22: Reduction of stiffness of the highlighted section, 1: Front supporting structure.

4 Results

This chapter presents a summary of the results obtained from the headform and the hybrid III dummy impact test. From Section 2.4, The threshold values referred are, HIC<1000 to avoid skull fracture, RIC<1.03 X 10^7 and PRHIC< 8.70 X 10^5 to avoid 50% probability of mTBI. Based on the data obtained from the simulation, HIC_{15}, RIC_{36} and $PRHIC_{36}$ are calculated and are presented in the following tables.

4.1 The free motion headform

Using the peak linear acceleration achieved at the CoG of the FMH during the bus model impact in different conditions the corresponding HIC_{15} is mentioned in Table 6. The peak linear acceleration values are mentioned in Table 17 in Appendix III.

Table 6: HIC_{15} for the FMH impact test

Free motion headform		**Velocity (km/h)**		
Height of head CoG from the ground (m)		**18**	**26**	**40**
	0.976	1137	3986	-
	1.096	710	2258	-
	1.576	468	1116	3011

4.2 The hybrid III 50th percentile male

Using the peak linear acceleration achieved at the CoG of the hybrid III dummy during the bus model impact in different conditions the corresponding HIC_{15} is mentioned in Table 7. The peak linear acceleration values are mentioned in Table 18 in Appendix III.

Table 7: HIC_{15} for the Hybrid III dummy impact test facing 0° to the bus for different simulated statures.

Hybrid III 50th percentile male		**Velocity (km/h)**	
Height of head CoG from the ground (m)		**18**	**26**
	0.976	1443	3944
	1.096	1365	3402
	1.576	512	1150

The RIC_{36} obtained from the rotational acceleration curve is mentioned in Table 8 and the peak rotational acceleration values are mentioned in Table 19 in Appendix III.

Table 8: RIC_{36} for the Hybrid III dummy impact test facing 0° to the bus

Hybrid III 50th percentile male		**Velocity (km/h)**	
Height of head CoG from the ground (m)		**18**	**26**
	0.976	1.15×10^8	1.76×10^8
	1.096	2.13×10^8	3.74×10^8
	1.576	8.86×10^7	4.06×10^7

The $PRHIC36$ also obtained from rotational acceleration along with mass of the head and second moment of inertia of the CoG of the head in the principal access is mentioned in Table 9 and the peak rotational acceleration values are mentioned in Table 19 in Appendix III.

Table 9: $PRHIC_{36}$ for the Hybrid III dummy impact test facing 0° to the bus

Hybrid III 50th percentile male		**Velocity (km/h)**	
Height of head CoG from the ground (m)		**18**	**26**
	0.976	4.15×10^6	1.92×10^7
	1.096	2.52×10^6	9.27×10^6
	1.576	5.62×10^4	9.42×10^4

Using the peak linear acceleration achieved at the CoG of the hybrid III dummy during the bus model impact in different conditions the corresponding $HIC15$ is mentioned in Table 10. The peak linear acceleration values are mentioned in Table 20 in Appendix III.

Table 10: HIC_{15} for the Hybrid III dummy impact test facing 90° to the bus

Hybrid III 50th percentile male		**Velocity (km/h)**	
Height of head CoG from the ground (m)		**18**	**26**
	0.976	68	547
	1.096	140	499
	1.576	99	361

The RIC36 obtained from the rotational acceleration curve is mentioned in Table 11 and the peak rotational acceleration values are mentioned in Table 21 in Appendix III.

Table 11: RIC_{36} for the Hybrid III dummy impact test facing 90° to the bus

Hybrid III 50th percentile male		**Velocity (km/h)**	
Height of head CoG from the ground (m)		**18**	**26**
	0.976	6.95×10^6	1.63×10^7
	1.096	1.03×10^7	3.80×10^7
	1.576	7.26×10^6	2.58×10^7

The PRHIC36 also obtained from rotational acceleration along with mass of the head and second moment of inertia of the CoG of the head in the principal access is mentioned in Table 12 and the peak rotational acceleration values are mentioned in Table 21 in Appendix III.

Table 12: $PRHIC_{36}$ for the Hybrid III dummy impact test facing 90° to the bus

Hybrid III 50th percentile male		**Velocity (km/h)**	
Height of head CoG from the ground (m)		**18**	**26**
	0.976	1.01×10^5	4.15×10^4
	1.096	4.42×10^5	2.44×10^6
	1.576	3.63×10^5	2.76×10^6

When the hybrid III dummy is facing the bus model at 0° and the height of the CoG of the head from the ground is 0.976m, the impact is on the front plastic panel.

When the thickness of the supporting steel structure which is right behind the front plastic panel is reduced from 4 mm to 0.1 mm, the comparison is shown in Table 13.

Table 13: Comparison of Injury criteria for different thickness of the supporting sheet metal

Thickness of the supporting sheet metal (mm)	**Peak linear acceleration (g's)**	**HIC_{15}**	**Peak rotational acceleration (rad/sec^2)**	**RIC_{36}**	**$PRHIC_{36}$**
0.1	254	2868	16320	1.43×10^8	1.32×10^7
4	305	3986	16590	1.76×10^8	1.92×10^7

5 Discussion

The Simulation of crash involving the bus model and the pedestrian model was performed using both FMH model and the Hybrid III dummy. The main reason for using the FMH model is to simulate the physical impact test suggested by the transport for London buses. HIC can be calculated from the FMH simulation. The HIC is a function of resultant linear acceleration reported at the CoG of FMH. It predicts skull fracture, and it is advised to have the value of HIC below 1000 to avoid the risk for skull fracture.

The injuries caused due to head impact is not only restricted to head injury due to skull fracture, but traumatic brain injuries also need to be considered. The TBI is caused due to the relative motion between the skull and brain. It is important to account rotational acceleration to calculate TBI's. The hybrid III dummy is used to perform the impact simulation to calculate rotational acceleration in addition to linear acceleration at the CoG of the head. The RIC is a function of resultant rotational acceleration and is a good predictor of mTBI's. The PRHIC is a function of rotational part of head impact power and is a good predictor of sTBI. The threshold value of RIC is 1.03×10^7 to avoid 50% probability of occurrence of mTBI. The threshold of PRHIC is 8.70×10^5 to avoid 50% probability of occurrence of mTBI. Further on, we can also compare the HIC values obtained from both the FMH impact simulation test and the hybrid III impact simulation test.

Simulation tests were run at different location, speed, and orientations.
The FMH impact with the bus model and the impact between Hybrid III dummy facing the bus model at 0° for the three different heights of head CoG from the ground, the value of HIC_{15} at 26 km/h and 40 km/h predicts high risk of skull fracture and at 18 km/h predicts low risk of skull fracture.

The hybrid III dummy while facing the bus model at 0° reports more than 50% probability of experiencing mTBI with the height of the head CoG from the ground at 1.576 m. At this CoG height the head was contacting the windscreen. As the height of the head CoG from the ground was set between 1.096 m to 0.976 m, there is more than 50% probability of experiencing sTBI as the head impacts the bus front end with steel reinforcements. This result was seen at both 18 km/h and 26 km/h of impact velocities.

Considering the most common scenario where the hybrid III dummy is facing at 90° to the bus model, risk of skull fracture was very low as the head does not seem to come in contact with the bus front structure. The reason for the dummy head not making contact with the bus is related to the kinematic movement of the dummy upper extremity that results in flexing of the neck and physical gap between the head and bus structure. High values of rotational acceleration are seen because of the larger travel of head CoG compared to the scenario where the hybrid III dummy facing the bus at 0°. At 18 km/h, probability of experiencing mTBI is close to 50%. At 26 km/h probability of experiencing sTBI is more than 50%. The behavior of injury criteria's is not consistent when the hybrid III dummy is at 90° to the bus, one possibility can be because of the absence of other body parts on the front part of the bus. The effect of this is seen in the results comparison when the height of head CoG from the ground is 0.976 m and when the height of the head CoG from the ground is 1.096 m and 1.576 m and the dummy model is at 90° to the bus model.

Reducing the stiffness of the front supporting structure saw little decrease in the injury criteria values. This shows that when the head is impact at the front structure, there needs to be an arrangement to decelerate the head before it rebounds. This will help in lowering the peak acceleration. However, doing this will compromise other bus properties that need the current stiffness in the bus front end. Typically, the properties governing the bus front structure design are strength, stiffness, and front impact safety demands.

The boundary conditions provided in the model does not include driver behaviour and the deceleration in case of braking. The material model used for the windscreen and the material model used for the front plastic parts had no failure criteria for most of the simulation tests run and is not validated with material tests. The confidence in the results achieved can only be improved when there is physical test data available, and the material model is refined based on the results obtained from the physical testing. From the physical testing, the boundary conditions can also be validated such as the friction coefficient values used between the bus and the dummy.

The run time of the one simulation is about 12 hours using 32 cores. Impact test was performed only on the vehicle centre of y axis. More tests need to be performed at different positions, as one of the common scenarios also include impact of the pedestrian at the edges of the bus.

The future work includes physical testing and validations of the material model, boundary conditions and test parameter validation, Impact testing at different positions along the bus front.

To build on the current thesis, it is important to perform physical testing of the materials in the bus and physical anthropometric test device, whose equivalent model is used in this thesis. The material models for windshield and bus front surface structure used in the thesis is not validated for crash test, hence failure mode of the windscreen and the plastic material model needs to be validated with physical material testing. The boundary conditions used for the simulations is based on the literature gathered, if we consider coefficient of friction value used between the front part of the bus and the dummy model, it is a constant, this can be further improved with physical test validation, where the friction value between the dummy model and different parts of the front part of the bus model is assigned. The impact simulations were performed along the vehicle centre of y-axis and the height was varied. Looking into crash databases in the future, there is a need to find more probable and accurate impact location crash severity is high.

6 References

1. [What is a 5th percentile female? – Idsemergencymanagement.com]
2. [ANTHROPOMETRY AND BIOMECHANICS (nasa.gov)]
3. Surrogate Head Forms for the Evaluation of Head Injury Risk Anna MacAlister Virginia Tech – Wake Forest University Center for Injury Biomechanics
4. Trosseille, X., C. Tarriere, F. Lavaste, F. Guillon, and A. Domont. (1992): *Development of a F.E.M. of the human head according to a specific test protocol*. In: Proceedings of 36th Stapp Car Crash Conference, SAE 922527, 1992
5. Hardy, W. N., C. D. Foster, M. J. Mason, K. H. Yang, A. I. King, and S. Tashman.(2001): *Investigation of head injury mechanisms using neutral density technology and highspeed biplanar X-ray*. Stapp Car Crash J. 45:337–368, 2001.
6. Kimpara, H., Y. Nakahira, M. Iwamoto, K. Miki, K. Ichihara, S. Kawano, and T. Taguchi.(2006): *Investigation of anteroposterior head-neck responses during severe frontal impacts using a brain-spinal cord complex FE model. Stapp Car Crash* J. 50:509–544, 2006.
7. Pellman, E. J., D. C. Viano, A. M. Tucker, I. R. Casson and J. F. Waeckerle.(2003): *Concussion in professional football: reconstruction of game impacts and injuries.* Neurosurgery 53:799–812; discussion 812–814, 2003.
8. Dokko, Y., R. Anderson, J. Manavis, P Blumburgs, J. McLean, L. Zhang, K. H. Yang, and A. I. King.(2003): *Validation of the human head FE model against pedestrian accident and its tentative application to the examination of the existing tolerance curve.* In: Proceedings of 18th International Technical Conference on the Enhanced Safety of Vehicles (ESV), Paper No. 322, 2003.
9. Gina Rablau (2016) *Calculus in crash safety: The head injury criterion (HIC) number*, pp 3-5
10. Zhan Xianghao,Li Yiheng,Liu Yuzhe,Domel August G.,Alizadeh Hossein Vahid,Raymond Samuel J.,Ruan Jesse,Barbat Saeed,Tiernan Stephen,Gevaert Olivier,Zeineh Michael M.,Grant Gerald A. and Camarillo David B. (2021) *The relationship between brain injury criteria and brain strain across different types of head impacts can be different.* J. R. Soc. Interface.**18**2021026020210260.
11. Charoenthong, S. and Carmai, J. (2014): *Finite Element Study of Post-crash Kinematics and Injury Mechanisms of Bus-Pedestrian Collisions* SAE Technical Paper 2014-01-2031, 2014, doi:10.4271/2014-01-2031.
12. Takhounts EG, Hasija V, Ridella SA, Rowson S, Duma SM.(2011*): Kinematic rotational brain injury criterion (BRIC).* In Proceedings of the 22nd enhanced safety of vehicles conference. Paper 2011 Jun 13 (No. 11-0263, pp. 1-10).
13. Takhounts EG, Craig MJ, Moorhouse K, McFadden J, Hasija V. (2013): *Development of brain injury criteria (BrIC).* SAE Technical Paper; 2013.
14. Kaveh Laksari, Michael Fanton, Lyndia C. Wu, Taylor H. Nguyen, Mehmet Kurt, Chiara Giordano, Eoin Kelly, Eoin O'Keeffe, Eugene Wallace, Colin Doherty, Matthew Campbell, Stephen Tiernan, Gerald Grant, Jesse Ruan, Saeed Barbat, and David B. Camarillo. (2020): *Journal of Neurotrauma*.Apr 2020.982-993.
15. Global status report on road safety 2018
16. National Center for Statistics and Analysis. (2020, December). *Overview of Motor Vehicle Crashes in 2019. (Traffic Safety Facts Research Note.* Report

No. DOT HS 813 060). Washington, DC: National Highway Traffic Safety Administration.
17. Large Truck and bus Crash Facts 2019, Federal Motor Carrier Safety Administration, Analysis Division, October 2021.
18. Guibing Li, Fang Wang, Dietmar Otte, Ciaran Simms. (2019): *Characteristics of pedestrian head injuries observed from real world collision data, Accident Analysis & Prevention, Volume 129,* 2019, Pages 362-366, ISSN 0001-4575.
19. John C. Gardiner PhD PE, and Check Y Kam MS PE (2011*): Break a leg: The ins and outs of analyzing pedestrian collisions.*
20. A. H. S. Holburn. (1943): Mechanics of head injuries. The Lancet - Neurology 2, 438-441. 1943.
21. Fahlstedt M, Depreitere B, Halldin P, Vander Sloten J, Kleiven S.(2015): *Correlation between injury pattern and Finite Element analysis in biomechanical reconstructions of Traumatic Brain Injuries*. J Biomech. 2015 May 1;48(7):1331-5. doi: 10.1016/j.jbiomech.2015.02.057. Epub 2015 Mar 12. PMID: 25817473.
22. https://www.scania.com/group/en/home/about-scania/scania-in-brief.html
23. London bus services limited, specification for new buses, Version 2.0. Issued March 2020.
24. London bus services limited, specification for new buses: Attachments, Version 2.0. Issued March 2020.
25. Charoenthong, S. and Carmai, J. (2014): *Finite Element Study of Post-crash Kinematics and Injury Mechanisms of Bus-Pedestrian Collisions* SAE Technical Paper 2014-01-2031, 2014, doi:10.4271/2014-01-2031.
26. Fahlstedt M, Depreitere B, Halldin P, Vander Sloten J, Kleiven S.(2015) *Correlation between injury pattern and Finite Element analysis in biomechanical reconstructions of Traumatic Brain Injuries.* J Biomech. 2015 May 1;48(7):1331-5. doi: 10.1016/j.jbiomech.2015.02.057. Epub 2015 Mar 12. PMID: 25817473.
27. European Commission (2021) Facts and Figures Buses / coaches / heavy goods vehicles. European Road Safety Observatory. Brussels, European Commission, Directorate General for Transport.
28. Road accidents in Inida 2020- *https://morth.nic.in/sites/default/files/RA_2020.pdf*
29. NEWMAN, J.A (2000): *A Proposed New Biomechanical Head Injury Assessment Function - The Maximum Power Index,* in: 44th Stapp Car Crash Conf., SAE Paper No. 2000-01-SC16.
30. Ommaya, A. K., P. Yarnell, A. Hirsch, and D. Harris (1967): *Scaling of experimental data on cerebral concussion in sub-human primates to concussive thresholds in man*. SAE 670906, 1967.
31. Hutchinson John, Kaiser.J Mark, Lankarani. M Hamid (1998): *The Head Injury Criterion (HIC) funcitonal,* Applied Mathematics and computaiton 96 Pg no.1-16.
32. Yong Han, Quan Li, Wei He, Fang Wann, Bingyu Wang, K.Mizuno (2017): *analysis of Vulnerable Road User Kinematics Before/During/After Vehicle Collisions Based on Video Records.* IRC-17-26.

7 Appendix I

Injury criteria evaluation

Aim:

To calculate Head injury criteria (HIC), Rotational Injury criteria (RIC) and Power rotational head injury criteria (PRHIC), when the 50th percentile hybrid III male dummy FE model is collided with rigid walls and different angles.

Background:

To calculate the injury criteria's, we need 6 DOF acceleration values at the head COG. The FE model setup contains Hybrid III dummy model in contact with the ground. A rigid wall is provided with the velocity of 5m/s.

1) Rigid wall-

- Dimension- 4000 × 2000 × 1 mm
- Material properties-

Table 14: Material properties of the rigid wall

Material Card	MAT20 MAT_RIGID
Density (kg/mm^3)	9.85×10^{-4}
Young's modulus (kN/mm^2 or Gpa)	210
Transnational Constraints	Along the y and z axis
Rotational Constraints	Along the x,y and z axis.

2) Ground-

- Dimension- 1000 × 1000 × 1
- Material properties-

Table 15: Material properties of the ground

Material Card	MAT20 MAT_RIGID
Density (kg/mm^3)	7.85×10^{-6}
Young's modulus (kN/mm^2 or Gpa)	210
Transnational Constraints	No constraints
Rotational Constraints	No constraints

Boundary conditions:

Based on the references [11], few initial boundary conditions are applied to the wall and dummy.

- Dummy- Friction between dummy and ground- 0.6
- Friction between wall and dummy- 0.3

Rigid Wall- Velocity of 5m/s (18kmph)

Method:

1. The Hybrid III 50% percentile male FE model is loaded along with the newly created rigid wall and ground. Suitable contact is provided, and friction is defined.
2. Node set on the rigid wall is created and velocity of 5m/s is initialized. Note- Contact with a rigid wall is provided only to the exterior surface of the dummy model and contact with ground is provided only to the foot.
3. The acceleration values are extracted, the units in which the values are stored are-
   i) Length unit- millimeter (mm)
   ii) Time unit- millisecond (ms)
   iii) Mass unit- kilogram (kg)
   iv) Force unit- kilonewton (kN)
4. **A** MATLAB code is generated to read the value and provide injury criteria value.

Results:

Table 16: Injury criteria values wrt. dummy position

Positioning (degrees)					
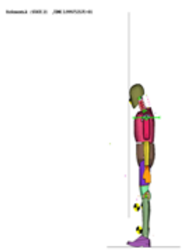					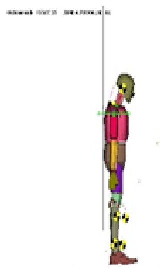
0	30	45	60	90	180
Peak linear acceleration (g's)					
228	210	194	194	29	187
Head injury criteria (HIC_{15})					
2479	1980	1663	1753	48	2058
Peak angular acceleration (radians/sec^2)					
8615.9	9445	10,831	15,257	5938.3	11,017
Rotational injury criteria (RIC_{36})					
$8.86 X 10^7$	1.43×10^8	1.86×10^8	1.14×10^8	8.65×10^6	7.86×10^7

Power rotational head injury criteria ($PRHIC_{36}$)					
4.96 X 10^4	1.19 × 10^4	1.69 × 10^4	2.15 × 10^4	2.41 × 10^5	4.73 × 10^5

Inference:

- From Table 16, it is seen that peak linear acceleration is highest when the pedestrian is directly facing the wall head on, and it decreases as the dummies angle is increased till it reaches 90 degrees where the peak linear acceleration is lowest. When the dummy is facing in the opposite direction of the bus i.e., 180 degrees, there is a rise in the peak linear acceleration.
- The HIC is maximum when the pedestrian is directly facing the wall head on and it decreases as the dummies angle is increased till it reaches 90 degrees. According to the result, the injury is highly severe and there is a high probability of skull fracture except when the pedestrian is facing 90 degrees to the wall.
- When it comes to peak angular acceleration, it is lower when the pedestrian is directly facing the wall head on, and it increases as the dummy's angle is increased till it reaches 60 degrees. At 90 degrees we see the lowest peak.
- The RIC is maximum when the pedestrian is facing 45 degrees to the wall and the value crosses the threshold at all the positions except when the pedestrian is facing 90 degrees to the wall. Predicting 50% probability of mTBI.
- It is seen that the PRHIC is maximum the dummy is facing in the opposite direction of the wall i.e., 180 degrees. But none of the values cross the threshold.
- It is strange to see such low values, when the dummy is at 90 degrees to the wall. The post-processing also shows no contact of the head with the wall during collision.

8 Appendix II

MATLAB Code

I. Calculation of HIC_{15} for the FMH impact test

```
clc;
clear all;
close all;
```

Loading the acceleration value from post processing

```
 load('Linear_acc.mat')
 % Time stamp in seconds
 Time= linear_accel(:,1)/1000;
 % Time stamp in milliseconds
 time= linear_accel(:,1);
 % Resultant linear acceleration in m/s2
 Lin_a=linear_accel(:,2)*1000;
 % Resultant linear acceleration in g's
 Lin_ag=linear_accel(:,2)*1000/9.81;
 % Velocity in x direction in mm/ms or m/s
 Lin_v_x= 5-linear_accel(:,3);
```

```
% Linear velocity plot
figure()
 plot (Time,Lin_v_x)
 grid on
 xlabel ('Time (sec)')
 ylabel ('Linear velocity (m/sec)')
 title ('Linear velocity in X (m/sec) vs Time (sec)')
 legend ('Linear velocity in X (m/sec) for dummy face 0^{o} to wall')
 count=0;

% Choosing the time stamp just when head velocity drop below zero
 for i=1:length(Time)
     if round(Lin_v_x(i),3)==0
        count=count+1;
     else
         break
     end
 end

% Choosing the time stamps required to calculate the HIC usually 4-36 milliseconds for
which we can get maximum HIC
 for j=4:36
 for i=count:length(Time)
    if round((Time(i)-Time(count)),3) == j/1000
        s(j)=i;
        break
    end
 end
end
```

```
% Using constant time gap but different starting point to find highest values of HIC
for j=1:36
for i=1:(length(time)-min(s(s>0)))
    if s(j)+i< length(time)
        % Calculating the area under graph to be used in evaluation of HIC
     area(j,i)=trapz(time(count+i:s(j)+i),Lin_ag(count+i:s(j)+i));
     a_bar(j,i)=area(j,i)/(time(s(j)+i)-time(count+i));
     HIC_1(j,i)=(Time(s(j)+i)-Time(count+i))*a_bar(j,i)^2.5;
    end
end
end


for j=1:36
for i=1:(length(time)-min(s(s>0)))
    if (HIC_1(j,i)== max(max(HIC_1)))
    add=i;
    l=j;
    break
end
end
end

HIC_max=max(max(HIC_1));

% Plotting of  Linear acceleration and highlighting the region considered to calculate
the HIC
figure()
plot(time,Lin_ag)
hold on
plot(time(count+add:s(l)+add),Lin_ag(count+add:s(l)+add),'LineWidth',2)
xlabel('Times(ms)')
ylabel('Linear acceleration (g)')
legend('Acceleration plot',sprintf('Maximum HIC region for time %d millisconds where
HIC= %f',l,HIC_max ))
```

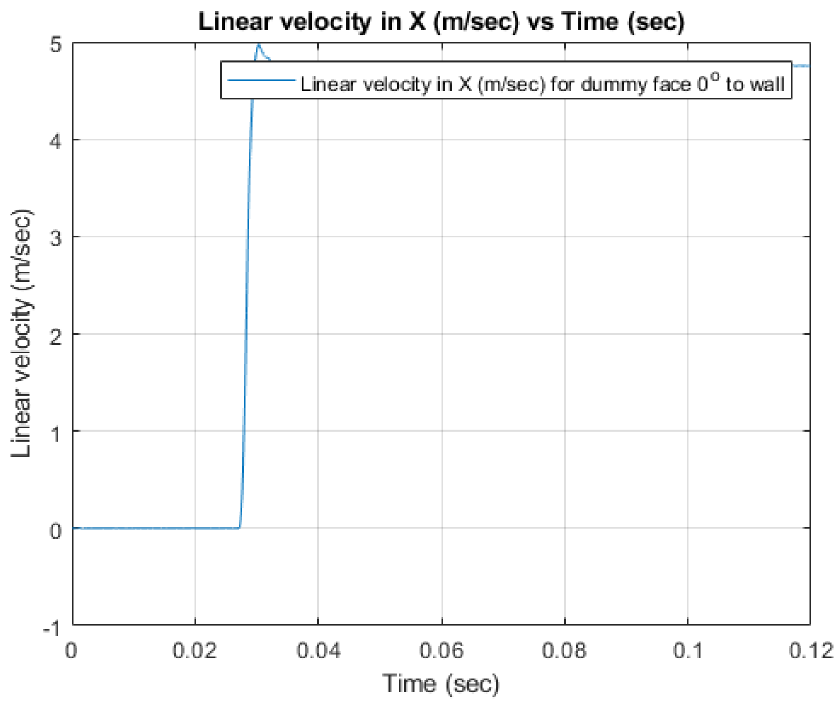

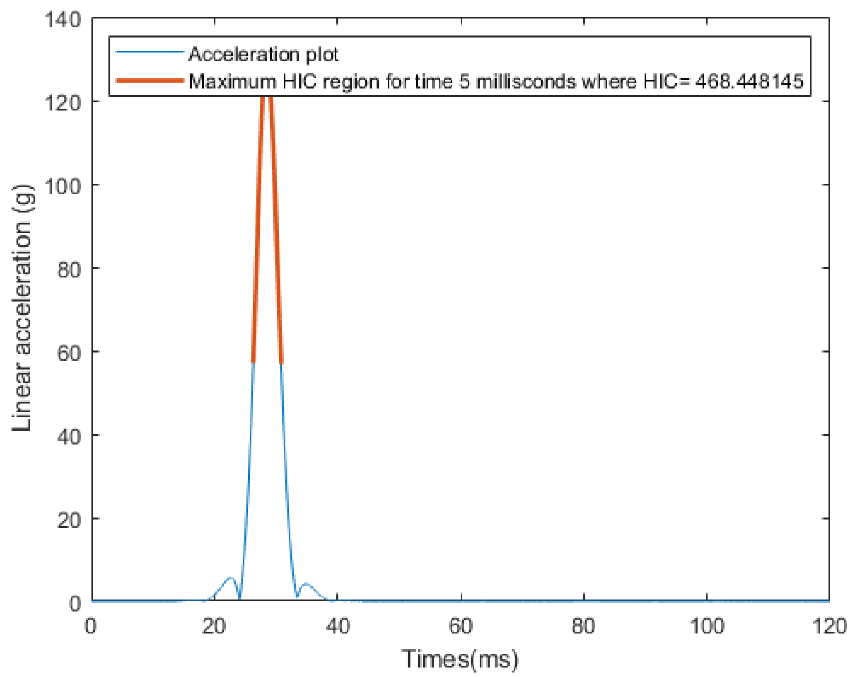

Published with MATLAB® R2021b

II. Calculation of HIC_{15} for the Hybrid III dummy impact test

```
clc;
clear all;
close all;
```

Loading the acceleration value from post processing

```
load('Linear_acc.mat')
% Time stamp in seconds
Time= linear_accel(:,1)/1000;
% Time stamp in milliseconds
time= linear_accel(:,1);
% Resultant linear acceleration in m/s2
Lin_a=linear_accel(:,2)*1000;
% Resultant linear acceleration in g's
Lin_ag=linear_accel(:,2)*1000/9.81;
% Velocity in x direction in mm/ms or m/s
Lin_v_x= linear_accel(:,3);
```

```
% Linear velocity plot
figure()
 plot (Time,Lin_v_x)
 grid on
 xlabel ('Time (sec)')
 ylabel ('Linear velocity (m/sec)')
 title ('Linear velocity in X (m/sec) vs Time (sec)')
 legend ('Linear velocity in X (m/sec) for dummy face 0^{o} to wall')
 count=0;

% Choosing the time stamp just when head velocity drop below zero
 for i=1:length(Time)
     if round(Lin_v_x(i),3)==0
        count=count+1;
     else
         break
     end
 end

% Choosing the time stamps required to calculate the HIC usually 4-36 milliseconds for
which we can get maximum HIC
 for j=4:36
 for i=count:length(Time)
    if round((Time(i)-Time(count)),3) == j/1000
        s(j)=i;
        break
    end
 end
end

% Using constant time gap but different starting point to find highest values of HIC
for j=1:36
for i=1:(length(time)-min(s(s>0)))
    if s(j)+i< length(time)
        % Calculating the area under graph to be used in evaluation of HIC
     area(j,i)=trapz(time(count+i:s(j)+i),Lin_ag(count+i:s(j)+i));
     a_bar(j,i)=area(j,i)/(time(s(j)+i)-time(count+i));
     HIC_1(j,i)=(Time(s(j)+i)-Time(count+i))*a_bar(j,i)^2.5;
    end
end
end


for j=1:36
for i=1:(length(time)-min(s(s>0)))
```

```
    if (HIC_1(j,i)== max(max(HIC_1)))
    add=i;
    l=j;
    break
end
end
end

HIC_max=max(max(HIC_1));

% Plotting of  Linear acceleration and highlighting the region considered to calculate
the HIC
figure()
plot(time,Lin_ag)
hold on
plot(time(count+add:s(l)+add),Lin_ag(count+add:s(l)+add),'LineWidth',2)
xlabel('Times(ms)')
ylabel('Linear acceleration (g)')
legend('Acceleration plot',sprintf('Maximum HIC region for time %d millisconds where
HIC= %f',l,HIC_max ))
```

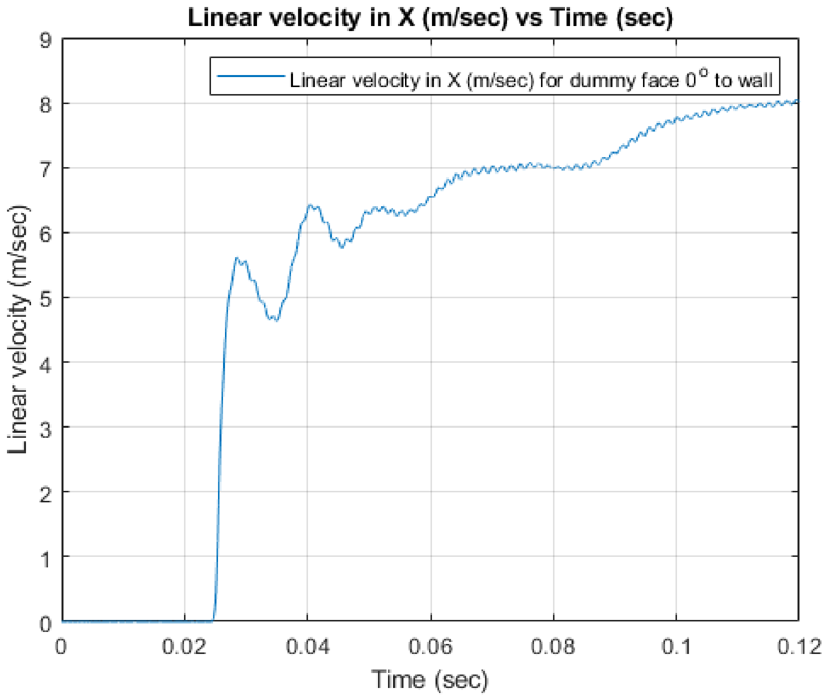

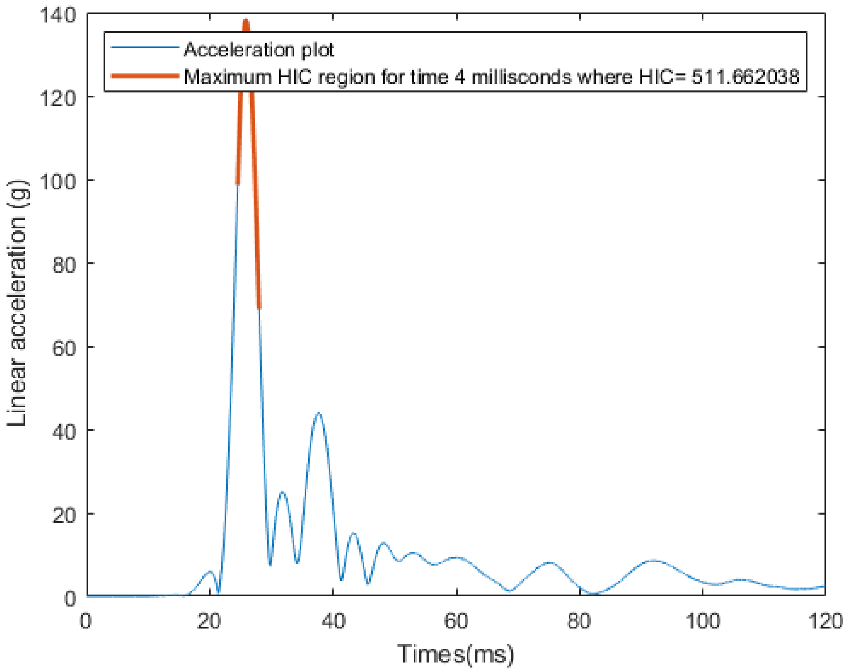

Published with MATLAB® R2021b

III. Calculation of RIC_{36} for the Hybrid III dummy impact test

```
clc;
clear all;
close all;
```

Loading the acceleration value from post processing

```
load('rot_val.mat')
% Time stamp in seconds
Time= rot_v(:,1)/1000;
% Resultant rotational acceleration in rad/sec2
r_a=rot_v(:,8).*10^6;
% Rotational velocity about Y direction in rad/sec
r_v_y=rot_v(:,3).*10^3;
```

```
% Rotaional velocity plot
figure()
 plot (Time,r_v_y)
 grid on
 xlabel ('Time (sec)')
 ylabel ('Rotational velocity (rad/sec)')
 title ('Rotational velocity (rad/sec) about Y vs Time (sec)')
 legend ('Rotational velocity (rad/sec) about Y for dummy face 0^{o} to wall')

% Choosing the time stamp just when head velocity drop below zero
 count=0;
 for i=1:length(Time)
     if round(r_v_y(i),3)==0
        count=count+1;
     else
```

```
            break
        end
    end

% Choosing the time stamps required to calculate the RIC usually 36 milliseconds
for i =count:length(Time)
    if round((Time(i)-Time(count)),3) == (36/1000)
        s=i;
        break
    end
end

 % Using constant time gap but different starting point to find highest values of RIC
for i=1:(length(Time)-min(s(s>0)))
    if s+i< length(Time)
     % Calculating the area under graph to be used in evaluation of RIC
     area(i)=trapz(Time(count+i:s+i),r_a(count+i:s+i));
     a_bar(i)=area(i)/(Time(s+i)-Time(count+i));
     RIC_1(i)=(Time(s+i)-Time(count+i))*a_bar(i)^2.5;
    end
end

for i=1:length(RIC_1)
    if (RIC_1(i)== max(RIC_1))
    add=i;
    break
end
end
RIC_max=max(RIC_1);

% Plotting of  Linear acceleration and highlighting the region considered to calculate
the RIC
figure()
plot(Time,r_a)
hold on
plot(Time(count+add:s+add),r_a(count+add:s+add),'LineWidth',2)
xlabel('Times(sec)')
ylabel('Rotational acceleration rad/sec^{2}')
legend('Acceleration plot',sprintf('Maximum RIC region for time 36 milliscונds where
RIC= %d',RIC_max))
```

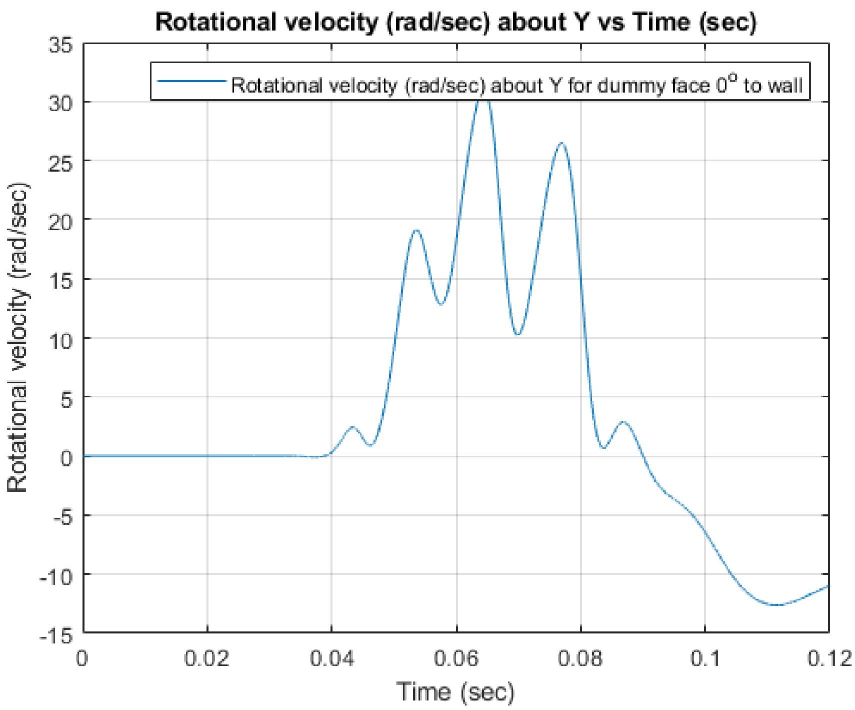

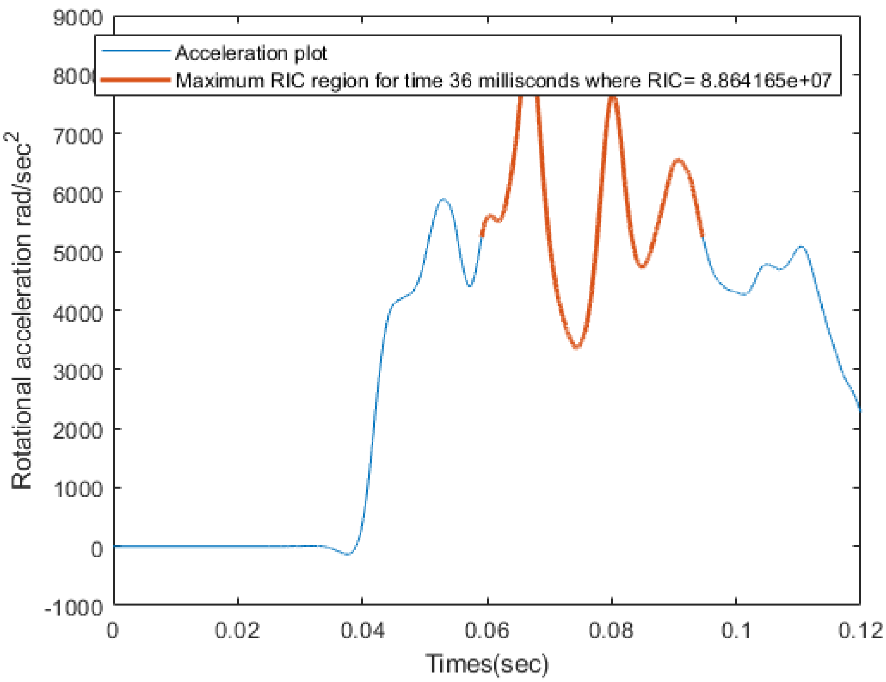

[Published with MATLAB® R2021b](https://www.mathworks.com/products/matlab)

IV. Calculation of PHIC36 for the Hybrid III dummy impact test

```
clc;
clear all;
close all;
```

```
% Mass of head in kg
m=4.5117;
% Principal moments of head inertia in x direction (kg.m^2)
```

```
I_xx=24526.1/10^6;
% Principal moments of head inertia in y direction (kg.m^2)
I_yy=22107.2/10^6;
% Principal moments of head inertia in z direction (kg.m^2)
I_zz=16355.2/10^6;

% Loading the rotational acceleration and velocity values from post processing
load('rot_val.mat')
% Time stamp in seconds
Time=rot_v(:,1)/1000;
% Rotational velocity in all the three direction in rad/msec
rx_v=rot_v(:,2);
ry_v=rot_v(:,3);
rz_v=rot_v(:,4);
% Rotational acceleration in all the three direction in rad/msec^2
rx_a=rot_v(:,5);
ry_a=rot_v(:,6);
rz_a=rot_v(:,7);
% Resultant Rotational acceleration in rad/msec^2
r_a=rot_v(:,8);

% Calculating the  rotational part of Head impact power (HIP), to be used in
calculation of PRHIC
% also called as rate of change in "angular head kinetic energy"
for i=1:length(Time)
    % Units- Kg.(m^2).(rad^2)/(sec^2)
    HIP_1(i,1)= I_xx*(rx_a(i)*10^6)*(rx_v(i)*10^3)+...
        I_yy*(ry_a(i)*10^6)*(ry_v(i)*10^3)+...
        I_zz*(rz_a(i)*10^6)*(rz_v(i)*10^3);
end

% figure()
% plot(Time, HIP_1)
```

Loading the acceleration value from post processing

```
load('Linear_acc.mat')
% Resultant linear acceleration in m/s2
 Lin_a=linear_accel(:,2)*1000;
 % Velocity in x direction in mm/ms or m/s
 Lin_v_x= linear_accel(:,3);

 % Calculating the linear velocity based on resultant linear acceleration in m/s
% lin_v=zeros(length(Time),1);
% for i=2:length(Time)
%     lin_v(i)=lin_v(i-1)- Lin_a(i)*(Time(i)-Time(i-1));
% end

% Linear velocity plot
figure()
 plot (Time,Lin_v_x)
 grid on
 xlabel ('Time (sec)')
 ylabel ('Linear velocity (m/sec)')
 title ('Linear velocity in x (m/sec) vs Time (sec)')
 legend ('Linear velocity in x (m/sec) for dummy face 0^{o} to wall')
 count=0;
```

```
% Choosing the time stamp just when head velocity drop below zero
 for i=1:length(Time)
     if round(Lin_v_x(i),3)==0
        count=count+1;
     else
         break
     end
 end

% Choosing the time stamps required to calculate the PRHIC usually 36 milliseconds
 for i =count:length(Time)
    if round((Time(i)*1000-Time(count)*1000)) == 36
        s=i;
        break
    end
end

% Using constant time gap but different starting point to find highest values of PRHIC
for i=1:(length(Time)-min(s(s>0)))
    if s+i< length(Time)
     % Calculating the area under graph to be used in evaluation of PRHIC
        area(i,1)=abs(trapz(Time(count+i:s+i),HIP_1(count+i:s+i)));
        a_bar(i,1)=area(i)/(Time(s+i)-Time(count+i));
        PRHIC_1(i,1)=((Time(s+i)-Time(count+i))*(a_bar(i)^2.5));
    end
end

for i=1:length(PRHIC_1)
    if (PRHIC_1(i)== max(PRHIC_1))
    add=i;
    break
end
end

PRHIC_max=max(PRHIC_1);

% Plotting of  Linear acceleration and highlighting the region considered to calculate
the PRHIC
figure()
plot(Time,r_a*10^6)
hold on
plot(Time(count+add:s+add),r_a(count+add:s+add).*10^6,'LineWidth',2)
xlabel('Times(sec)')
ylabel('Rotational acceleration (rad/sec^{2})')
legend('Acceleration plot',sprintf('Maximum PRHIC region for time 36 millisconds where
PRHIC=%d',PRHIC_max))
```

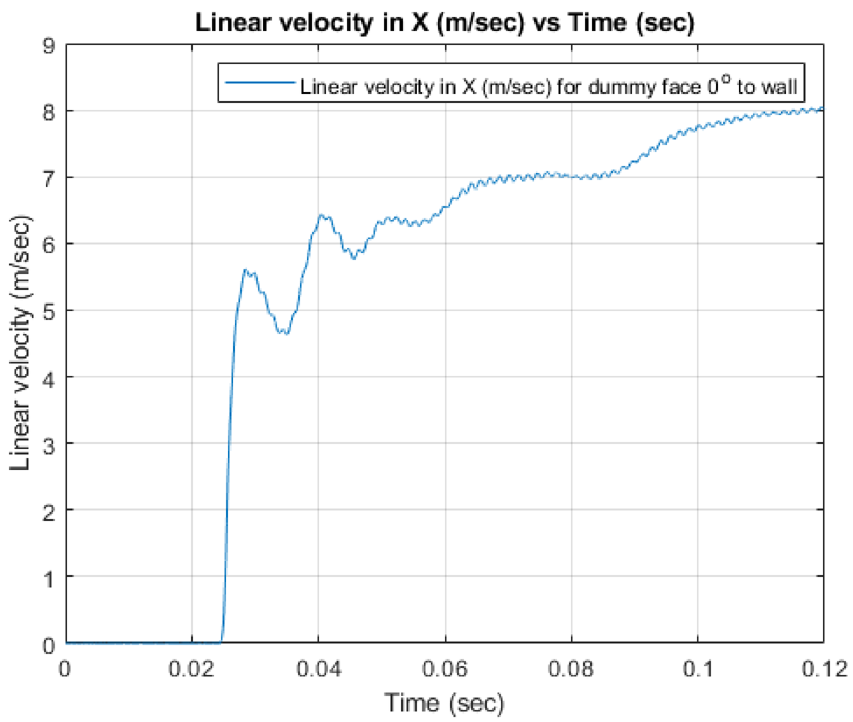

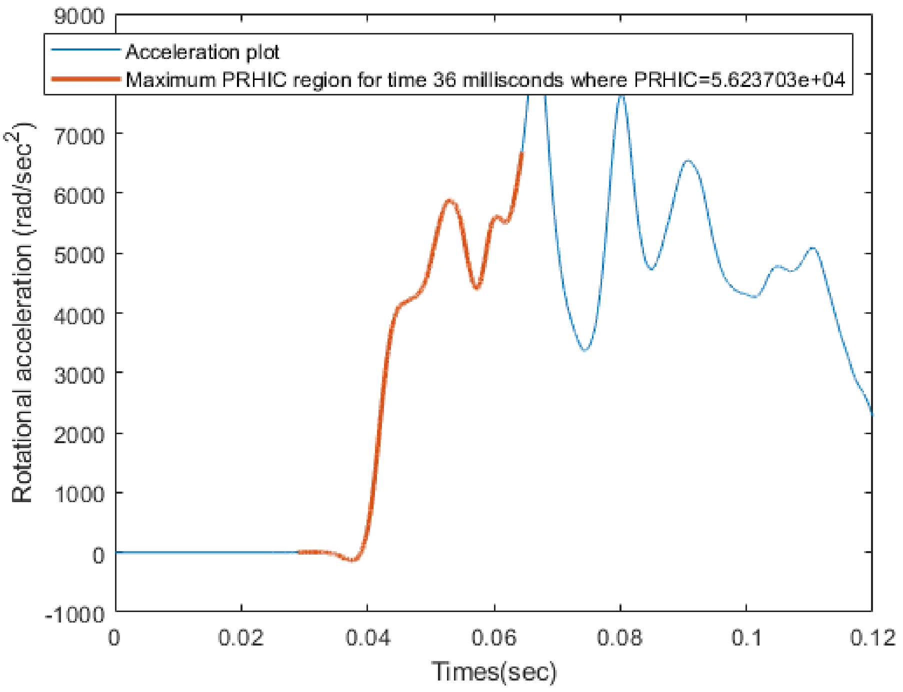

Published with MATLAB® R2021b

V. Force Vs. Discplacement plot

```
clc;
clear all;
close all;
```

FMH

```
figure()
load('F_n_D.mat')
plot (FMH(:,1),FMH(:,2),'r','LineWidth',2)
hold on
xlabel ('Displacement (mm)');
ylabel ('Force (kN)');
title ('Force Vs Displacement');
```

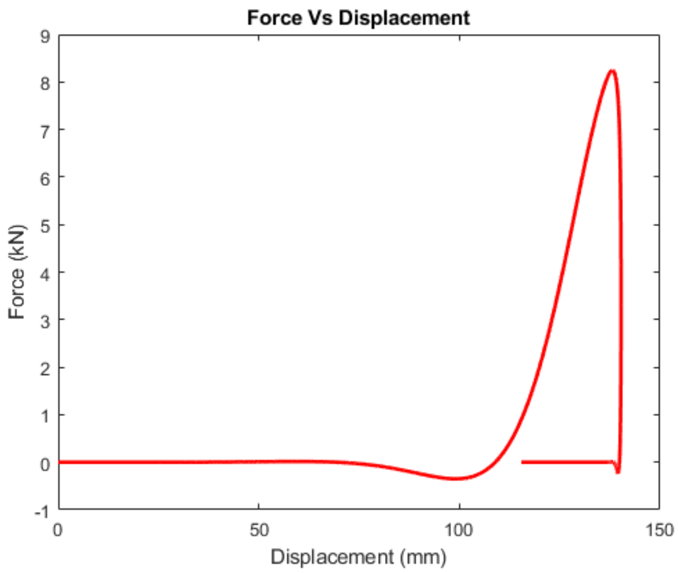

Hybrid III 50th percentile male

```
load('F_n_D_hybridd_III.mat')
plot (FMH(:,1),FMH(:,2),'b')
legend ('Free motion headform','Hybrid III 50^{th} percentile male')
```

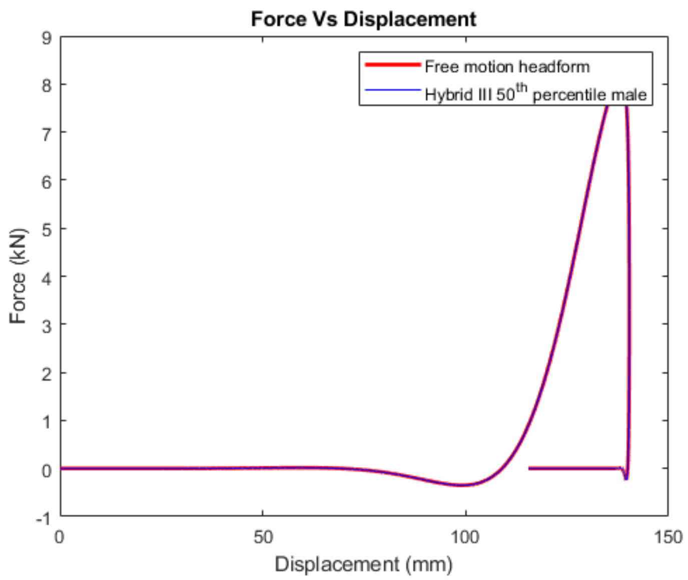

Published with MATLAB® R2021b

9 APPENDIX III

9.1 Peak Linear acceleration

The peak linear acceleration achieved at the CoG of the FMH during the bus model impact in different conditions is mentioned in Table 11.

Table 17: Peak linear acceleration (in g's) of the head CoG from the FMH impact test

Free motion headform		**Velocity (km/h)**		
Height of head CoG from the ground (m)		**18**	**26**	**40**
	0.976	175	261	-
	1.096	144	237	-
	1.576	129	182	267

When the dummy is facing the bus at 0°, The peak linear acceleration achieved at the CoG of the head of the hybrid III dummy during the bus model impact in different conditions is mentioned in Table 18.

Table 18: Peak linear acceleration (in g's) of the head CoG from the Hybrid III dummy impact test facing 0° to the bus

Hybrid III 50th percentile male		**Velocity (km/h)**	
Height of head CoG from the ground (m)		**18**	**26**
	0.976	196	306
	1.096	191	292
	1.576	135	182

When the dummy is facing the bus model at 90°, The peak linear acceleration achieved at the CoG of the head of the hybrid III dummy during the bus impact in different conditions is mentioned in Table 19.

Table 19: Peak linear acceleration of the head CoG from the Hybrid III dummy impact test facing 90° to the bus

Hybrid III 50th percentile male		**Velocity (km/h)**	
Height of head CoG from the ground (m)		**18**	**26**

	0.976	32	128
	1.096	46	84
	1.576	37	71

9.2 Peak Rotational acceleration

When the dummy is facing the bus at 0°, The peak rotational acceleration achieved at the CoG of the head of the hybrid III dummy during the bus model impact in different conditions is mentioned in Table 20.

Table 20: Peak rotational acceleration of the head CoG from the Hybrid III dummy impact test facing 0° to the bus

Hybrid III 50th percentile male		**Velocity (km/h)**	
Height of head CoG from the ground (m)		**18**	**26**
	0.976	12910	16590
	1.096	18200	24660
	1.576	4821	6400

When the dummy is facing the bus at 90°, The peak rotational acceleration achieved at the CoG of the head of the hybrid III dummy during the bus model impact in different conditions is mentioned in Table 21.

Table 21: Peak rotational acceleration of the head CoG from the Hybrid III dummy impact test facing 90° to the bus

Hybrid III 50th percentile male		**Velocity (km/h)**	
Height of head CoG from the ground (m)		**18**	**26**
	0.976	3853	8272
	1.096	5560	9558
	1.576	5781	10900

9.3 FMH Impact test with failure mode enabled for windscreen

Figure 23 shows the impact between the FMH and the bus model, where the point of contact is at the windscreen. The height of the head CoG from the ground is 1.576m and the impact velocity is 26 km/h.

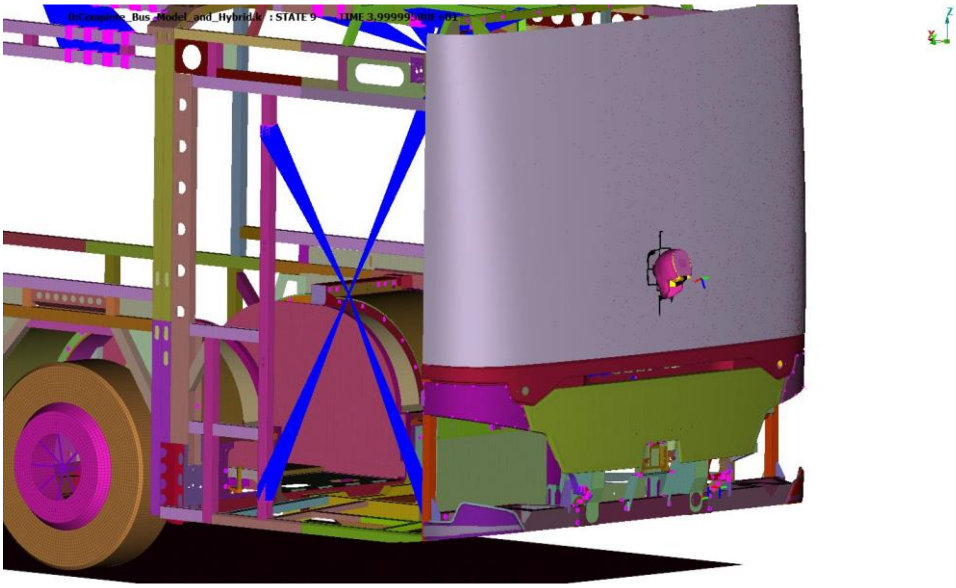

Figure 23: FMH impact with windscreen. Failure mode of the material enabled.

Hybrid III dummy Impact test with failure mode enabled for windscreen

Figure 24 shows the impact between the hybrid III dummy and the bus model, where the point of contact is at the windscreen. The height of the head CoG from the ground is 1.576m and the impact velocity is 26 km/h.

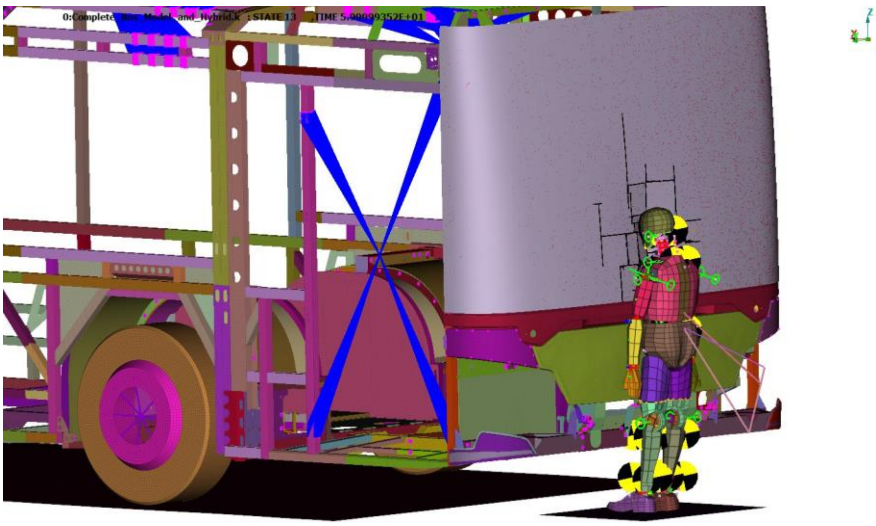

Figure 24: Hybrid III dummy impact with windscreen. Failure mode of the material enabled.

Results

Table 22: Comparison of Peak linear acceleration and HIC_{15} from the impact test of FMH and hybrid III dummy

	Peak linear acceleration (g's)	HIC_{15}
FMH	85.66	209.62
Hybrid III	85.07	364.64

Table 23: Peak rotational acceleration, RIC_{36} and $PRHIC_{36}$ from the impact test of hybrid III dummy

	Peak rotational acceleration (rad/sec^2)	RIC_{36}	$PRHIC_{36}$
Hybrid III	6413	1.22×10^7	6.94×10^3

Discussion

The results show low probability of skull fracture based on HIC_{15}. There is 50% probability of the occurrence of mTBI based on RIC_{36}. When this test is compared to the test where the material model had no failure mode activated, it is seen that the peak linear acceleration drops by 55% whereas the peak rotational acceleration remains same. Since the material cracks and the head travels for a longer time, the injury criteria values are low. The material model needs more research to improve the model. Also, data from actual physical test is required to validate the simulation result.

DEPARTMENT OF MECHANICS AND
MARITOME SCIENCES
CHALMERS UNIVERSITY OF TECHNOLOGY
Gothenburg, Sweden 2022
www.chalmers.se

CHALMERS
UNIVERSITY OF TECHNOLOGY